TABLE 1
Sequences of quantitative RT-PCR primers

Probe	Primer 1	Primer 2
FAS	5'-tgctcccagctgcaggc-3'	5'-gcccggtagctctgggtgta-3'
SCD-1	5'-tgggttggctgcttgtg-3'	5'-gcgtgggcaggatgaag-3'
SREBP1c	5'-catggattgcacatttgaag-3'	5'-cctgtgtcccctgtctca-3'
FAT	5'-tggctaaatgagactgggacc-3'	5'- acatcaccactccaatcccaag-3'
MCAD	5'-tcgaaagcggctcacaagcag-3'	5'-caccgcagctttccggaatgt-3'
UCP2	5'-cattctgaccatggtgcgtactga-3'	5'-gttcatgtatctcgtcttgaccac-3'
PPAR-α	5'-ggatgtcacacaatgcaattcgc-3'	5'-tcacagaacggcttcctcaggt-3'
PEPCK	5'-agcggatatggtgggaac-3'	5'-ggtctccactccttgttc-3'
G6Pase	5'-aaagagactgtgggcatcaatc-3'	5'-aatgcctgacaagactccagcc-3'
GAPDH	5'-accacagtccatgccatcac-3'	5'-tccaccaccctgttgctgta-3'

FAS, fatty acid synthase; SCD1, stearoyl-CoA desaturase 1; FAT, fatty acid transporter; MCAD, medium-chain acyl-CoA dehydrogenase; PEPCK, phosphoenolpyruvate carboxylase; G6Pase, glucose-6-phosphatase; GAPDH, glyceraldehyde-3-dehydrogenase.

dynamically, in response to the energy balance. We reported that hepatic AKT activation resulted in marked alterations in glucose and lipid metabolism (9), suggesting that the liver is a potential site of ectopic expression. We herein expressed UCP1 protein in the liver, before or after diabetes associated with dietary obesity had developed. We found that hepatic UCP1 expression improved diabetes and obesity under high-fat diet conditions through local effects in the liver as well as remote effects in adipose tissues, muscle, and the hypothalamus. However, in standard diet–fed lean mice, effects on glucose and lipid metabolism were minimal. Using gene transduction after disease development, as in this study, provides useful information allowing analysis of therapeutic, rather than preventive, effects that would be difficult to examine using congenitally gene-engineered animal models.

RESEARCH DESIGN AND METHODS

Preparation of recombinant adenovirus. Murine UCP1 cDNA (10) was provided by Professor Leslie P. Kozak (Pennington Biomedical Research Center). Murine liver carnitine palmitoyltransferase 1 (CPT1a) cDNA was obtained by RT-PCR with liver total RNA and primers designed from the reported sequence (GenBank accession no. NM_013495). Recombinant adenovirus, containing murine UCP1 (11) or CPT1a cDNA under the CAG promoter, was prepared as described previously (12). A recombinant adenovirus bearing the bacterial β-galactosidase gene (*Adex1CAlacZ*) (13) was used as a control.

Animals. Animal studies were conducted under protocols in accordance with the institutional guidelines for animal experiments at Tohoku University. Male C57BL/6N mice were housed individually and divided into high-fat diet (32% safflower oil, 33.1% casein, 17.6% sucrose, and 5.6% cellulose [14]) and standard diet (65% carbohydrate, 4% fat, and 24% protein) groups at 5 weeks of age, when body weights were 21.2 ± 0.25 g (means ± SE). Four weeks after separation, body weight–matched mice for each group received an injection of adenovirus via the tail vein. Viruses were administered intravenously at a dose of 2×10^8 plaque-forming units. For pair-feeding experiments, after 4 weeks of high-fat diet, mice were allotted into three groups. Two groups of mice received an injection of UCP1 or LacZ adenovirus. After 24 h, mice in the third group received an injection of LacZ adenovirus. The latter LacZ mice were given their daily food allotments on the basis of the previous day's consumption by UCP1 mice.

Antibodies. UCP1, acetyl-CoA carboxylase 1 (ACC 1), and insulin receptor antibodies were purchased from Santa Cruz Biotechnology (Santa Cruz, CA). The α-subunit of AMP-activated protein kinase (AMPK), phospho-AMPK (Thr172), and phospho-ACC (Ser79) antibodies were purchased from Cell Signaling Technology (Beverly, MA). Affinity-purified antibody against insulin receptor substrate 1 (IRS1) was prepared as described previously (15).

Immunoblotting. Tissue samples were prepared as previously described (9), and tissue protein extracts (250 μg of total protein) were boiled in Laemmli buffer that contained 10 mmol/l dithiothreitol and subjected to SDS-PAGE. The immunoblots were visualized with an enhanced chemiluminescence detection kit (Amersham, Buckinghamshire, U.K.).

Triglyceride content of the liver. Frozen livers were homogenized, and triglycerides were extracted with $CHCl_3$:CH_3OH (2:1, vol:vol), dried, and resuspended in 2-propanol (16). Triglyceride contents were measured using Lipidos liquid (TOYOBO, Osaka, Japan).

Oxygen consumption. Oxygen consumption was measured with an O_2/CO_2 metabolism measuring system (model MK-5000RQ; Muromachikikai, Tokyo, Japan). Each mouse was kept unrestrained in a sealed chamber with an air flow of 0.5 l/min for 5 h at 25°C without food or water during the light cycle. Air was sampled every 3 min, and the consumed oxygen concentration (Vo_2) was calculated.

Histological analysis. Livers as well as epididymal fat (white adipose tissue) and brown adipose tissues were removed and fixed with 10% formalin and embedded in paraffin. Tissue sections were stained with hematoxylin and eosin. Total adipocyte areas were traced manually and analyzed. Brown and white adipocyte areas were measured in 100 or more cells per mouse in each group.

Measurement of body temperature. Rectal temperature was measured with a Thermalert TH-5 (Physitemp, Clifton, NJ).

Measurement of ATP. The ATP levels in liver homogenates were measured with a luciferase-luciferin system (17) by using an ATP determination kit (Molecular Probes, Eugene, OR).

Measurement of AMPK activity. Livers were homogenized, and aliquots of supernatant were incubated with anti-AMPK α-subunit antibody. AMPK activity in the immunoprecipitates was assessed as a function of SAMS peptide phosphorylation, as previously described (18).

Tyrosine phosphorylation of insulin receptor and IRS1. Mice that were fasted for 16 h received an injection of 100 μl of normal saline (0.9% NaCl), with or without 10 units/kg body wt insulin, via the tail vein. Hindlimb muscles were removed 300 s later and immediately homogenated. After centrifugation, the resultant supernatants were used for immunoprecipitation with anti–insulin receptor or anti-IRS1 antibody. Immunoprecipitates were subjected to SDS-PAGE and then immunoblotted using anti-phosphotyrosine antibody (4G10) or individual antibodies as described previously (15).

Blood analysis. Blood glucose was assayed with Antsense II (Horiba Industry, Kyoto, Japan). Serum insulin and leptin were determined with ELISA kits (Morinaga Institute of Biological Science, Yokohama, Japan). Serum adiponectin and tumor necrosis factor-α (TNF-α) concentrations were measured with an ELISA kit (Ohtsuka Pharmaceutical, Tokyo, Japan) and a TNF-α assay kit (Amersham Biosciences, Uppsala, Sweden), respectively. Serum total cholesterol, triglyceride, and free fatty acid concentrations were determined with a Cholescolor liquid, Lipidos liquid (TOYOBO), and NEFA C (Wako Pure Chemical, Osaka, Japan) kits, respectively.

Glucose, insulin, and leptin tolerance tests. Glucose tolerance tests were performed on fasted (10 h) mice. Mice were given oral glucose (2 g/kg body wt), and blood glucose was assayed immediately before and at 15, 30, 60, and 120 min after administration. Insulin tolerance tests were performed on fed mice. Mice received an injection of human regular insulin (0.75 units/kg body wt; Eli Lilly, Kobe, Japan) into the intraperitoneal space, and blood glucose was assayed immediately before and at 20, 40, 60, and 80 min after injection. Leptin tolerance tests were performed as reported previously (19) with slight modification. Fasted (12 h) mice received an injection of mouse leptin (7.2 mg/kg body wt; R&D Systems) into the intraperitoneal space, and food intake amounts for 12 h thereafter were determined. Ratios of food intake amounts to those of vehicle-injected mice were calculated.

Quantitative RT-PCR–based gene expression. Total RNA was isolated from 0.1 g of mouse hepatic tissue with ISOGEN (Wako Pure Chemical), and

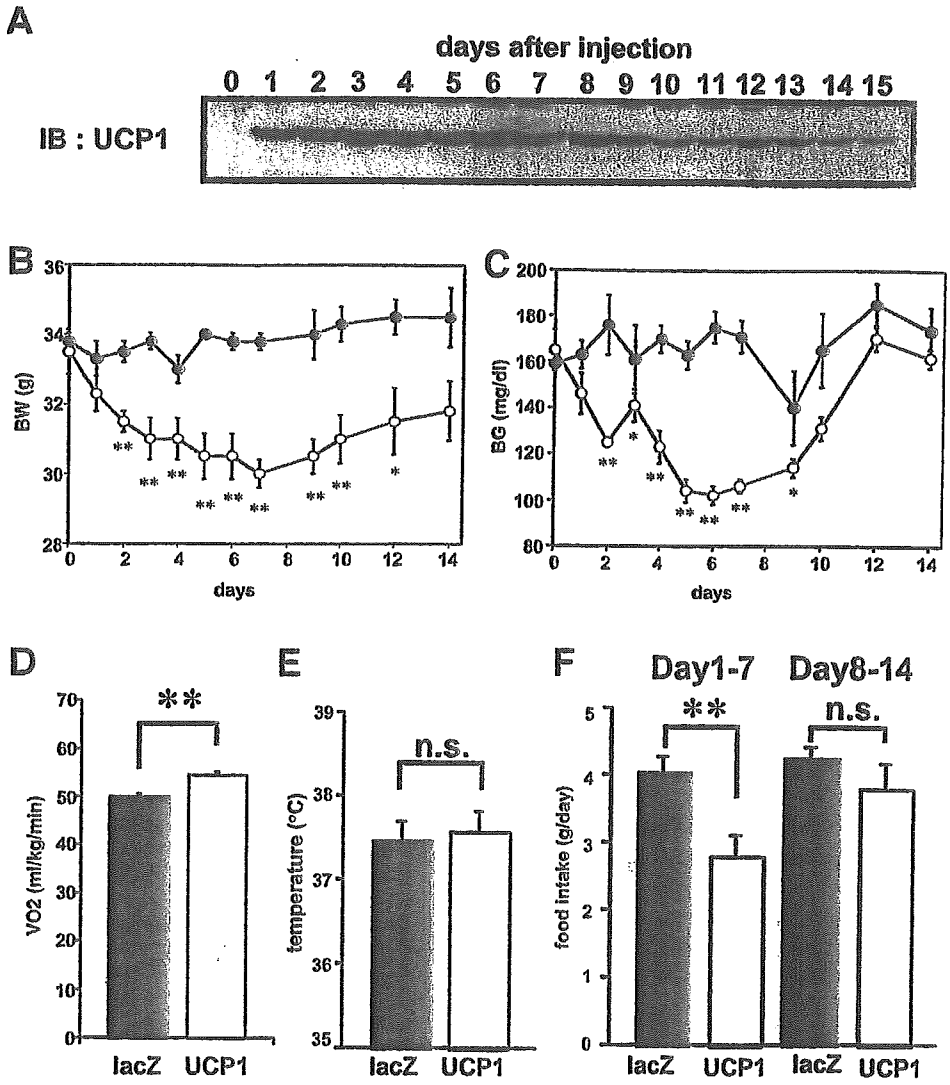

FIG. 1. Hepatic UCP1 expression reduced body weight and blood glucose levels. *A*: Ectopic UCP1 expression in the liver in high-fat–fed mice was detected by immunoblotting of hepatic extracts (250 μg total protein/lane). Liver samples were collected at different times after adenovirus injection. *B* and *C*: Body weights (*B*) and blood glucose levels (*C*) in the ad libitum–fed state after adenoviral administration in control (LacZ) mice (●) and UCP1 mice (○; $n = 4$ per group). *D*: Resting Vo_2 was measured on day 3 after adenoviral injection with open-circuit indirect calorimetry. All mice were kept in a cage for ~5 h in the daytime without food or water ($n = 5$ per group). *E*: Rectal temperature was measured in the ad libitum–fed state on day 7 after adenoviral injection ($n = 6$ per group). *F*: Average daily food intake amounts over the first and the second weeks after adenoviral administration are presented. Regarding all panels, similar results were obtained from 10 or more experiments, and representative results are presented as means ± SE. *$P < 0.05$, **$P < 0.01$ assessed by unpaired t test.

cDNA synthesis was performed with a Cloned AMV First Strand Synthesis Kit (Invitrogen, Rockville, MD) using 5 μg of total RNA. cDNA synthesized from total RNA was evaluated in a real-time PCR quantitative system (Light Cycler Quick System 350S; Roche Diagnostics, Mannheim, Germany). The relative amount of mRNA was calculated with glyceraldehyde-3-dehydrogenase mRNA as the invariant control. The primers used are described in Table 1.

All data were expressed as means ± SE. The statistical significance of differences was assessed by the unpaired t test and one-factor ANOVA.

RESULTS

Hepatic UCP1 expression increased energy expenditure and reduced body weight and blood glucose levels in mice that had high-fat diet–induced obesity and diabetes. C57BL/6 mice were on a high-fat diet for 4 weeks, resulting in diabetes associated with obesity. The UCP1 adenovirus vector (11) was then administered intravenously (UCP1 mice). Mice that were given the LacZ adenovirus were used as a control (LacZ mice). No significant alterations were observed in body weights (Fig. 1*B*), blood glucose levels (Fig. 1*C*), food intake amounts, body temperature, or plasma lipid parameters (data not shown) before versus after LacZ adenovirus administration. Systemic infusion of recombinant adenoviruses into mice through the tail vein primarily resulted in expression of transgenes in the liver, with no detectable expression in peripheral tissues such as muscle, fat, kidney, or brain (data not shown), as reported previously (20). As shown in Fig. 1*A*, immunoblotting revealed that ectopic UCP1 expression in the liver peaked on day 3. Maximal expression was maintained through day 8. After day 9, hepatic expression of UCP1 decreased, and very small amounts of UCP1 protein were detected on day 14 (Fig. 1*A*).

In UCP1 mice, body weight and blood glucose levels were markedly decreased (Fig. 1*B* and *C*) concomitantly with hepatic expression levels of UCP1. On day 7, body weights of UCP1 mice were significantly lower, by 13%, than those of control mice. After day 9, body weight and

blood glucose levels began to increase as the expression of hepatic UCP1 declined. These findings indicate that hepatic UCP1 expression exerted therapeutic effects on diabetes associated with diet-induced obesity.

Resting oxygen consumption on day 3 was markedly increased, by 12%, in UCP1 mice compared with controls (Fig. 1*D*), whereas rectal temperature did not differ between the two (Fig. 1*E*). Thus, ectopic UCP1 in the liver, like endogenous UCP1 in brown adipocytes, promoted inefficient metabolism, thereby enhancing energy expenditure and leading to weight reduction. This effect, however, was not sufficient to raise whole-body temperature. In addition, hepatic UCP1 expression changed food intake. Whereas without hepatic UCP1 expression, food intake amounts in high-fat–fed mice were markedly increased compared with those in standard diet–fed lean mice (compare Figs. 1*F* and 5*D*), hepatic UCP1 expression reversed hyperphagia in mice with high-fat diet–induced obesity and diabetes (Fig. 1*F*). After day 8, concomitantly with the drop in hepatic UCP1 expression, hyperphagia was restored (Fig. 1*F*). In contrast, mice received an intravenous injection of adenovirus encoding CPT1a, another mitochondrial protein, did not show significantly altered food consumption (data not shown), suggesting that food intake suppression induced by hepatic UCP1 expression is not a nonspecific effect of expression of any of the hepatic mitochondrial proteins.

To eliminate any secondary effects of reduced food intake induced by hepatic UCP1 expression, we performed pair-feeding experiments. In contrast to UCP1 mice, pair-fed LacZ mice exhibited only slight decreases in body weights and blood glucose levels (of 3.1 and 6.9%, respectively, on day 7 after adenoviral administration). These results suggest that increased energy expenditure is an important mechanism underlying marked improvements of obesity and diabetes in UCP1 mice.

Hepatic UCP1 expression decreased fat contents in the liver and adipose tissues. Hepatic and adipose fat accumulations were examined on day 7 after adenoviral gene delivery. In the high-fat–fed control mice, liver weight and triglyceride content were markedly increased compared with the standard chow–fed lean mice (compare Fig. 2*A* and *B* with Fig. 5*E* and *F*, respectively). Hepatic UCP1 expression significantly decreased liver weight (Fig. 2*A*) and triglyceride content (Fig. 2*B*) compared with LacZ mice, with high-fat feeding. It is interesting that hepatic UCP1 expression also decreased fat content in their adipose tissues. For example, epididymal fat weight was significantly decreased in UCP1 mice compared with that in controls (Fig. 2*C*). Thus, hepatic expression of UCP1 exerts not only local effects in the liver but also remote effects on metabolism in other tissues.

These results were confirmed by the histological findings. No apparent infiltration or structural change was observed in the livers of either LacZ mice or UCP1 mice, indicating the absence of adenovirus-induced liver damage (Fig. 2*D*). Whereas abundant lipid droplets were present in the livers of control mice, these lipid droplets were markedly diminished in UCP1 mouse livers, indicating marked improvement of fatty liver findings in response to UCP1 expression (Fig. 2*D*). Furthermore, the cell diameters in epididymal fat (Fig. 2*E*) and brown adipose (Fig. 2*F*) tissues were significantly decreased in UCP1 mice. Expression levels of endogenous UCP1 protein in brown adipocytes were similar in the two groups (Fig. 2*G*), suggesting that energy expenditure in brown adipocytes was not increased in UCP1 mice. These findings suggest that hepatic UCP1 expression promotes hydrolysis of triglycerides already stored in adipose tissues, leading to smaller adipocytes with the resultant fatty acids being mobilized and metabolized as a substrate for oxidation in the liver.

Hepatic expressions of enzymes involved in lipid metabolism and glucose production. To elucidate the underlying mechanism whereby stored fat was decreased in the liver by hepatic UCP1 expression, we examined the expressions of proteins involved in lipid metabolism by quantitative RT-PCR. Significant reductions in the expressions of the lipogenic enzymes, including stearoyl-CoA desaturase-1 and fatty acid synthase, were observed in UCP1 mice (Fig. 3*A*). Sterol regulatory element binding protein 1c (SREBP1c) expression in the liver tended to be diminished. In contrast, hepatic expressions of enzymes involved in fatty acid oxidation tended to be increased. In particular, expressions of fatty acid transporter and UCP2 were significantly increased (Fig. 3*B*).

We further examined expression levels of key enzymes for hepatic glucose production. Hepatic phosphoenolpyruvate carboxykinase and glucose-6-phosphatase expressions were significantly decreased in UCP1 mice (Fig. 3*C*), suggesting a decrease to contribute to improvement of diabetes.

UCP1 expression may activate AMPK as a result of decreased generation of ATP. AMPK activation reportedly decreases malonyl-CoA generation via inhibition of ACC (21), resulting in enhancement of fatty acid oxidation. Therefore, ATP levels and AMPK phosphorylation in the liver were examined in LacZ and UCP1 mice under ad libitum feeding conditions. Hepatic ATP concentrations in UCP1 mice were approximately half those in control mice (Fig. 3*D*) but still ~2.3-fold those in standard diet–fed control mice. Hepatic AMPK activity was increased 1.6-fold in UCP1 mice compared with LacZ mice (Fig. 3*E*). The phosphorylation state of the α-subunit of AMPK in the liver was enhanced in UCP1 mice (Fig. 3*F*). Furthermore, resultant enhancement of hepatic ACC phosphorylation was observed (Fig. 3*G*). These findings suggest that AMPK activation induced by UCP1 expression plays an important role in the observed marked improvement of fatty liver findings via enhanced fatty acid oxidation.

Glucose and lipid metabolism in UCP1 mice. The results of oral glucose tolerance (Fig. 4*A*) and insulin tolerance (Fig. 4*B*) tests on day 7 after adenoviral administration clearly showed that hepatic expression of UCP1 markedly improved glucose tolerance and insulin sensitivity in obese and diabetic mice. Improved insulin sensitivity in muscle was confirmed by enhanced insulin receptor and IRS1 phosphorylation (Fig. 4*C*) in response to insulin administration. Thus, hepatic UCP1 expression exerts a remote beneficial effect on insulin sensitivity in muscle.

In addition, plasma lipid parameters were decreased in UCP1 mice. Total plasma cholesterol levels tended to be decreased in UCP1 mice compared with controls, although the changes were not statistically significant (Fig. 4*D*). Plasma triglyceride and free fatty acid levels were signifi-

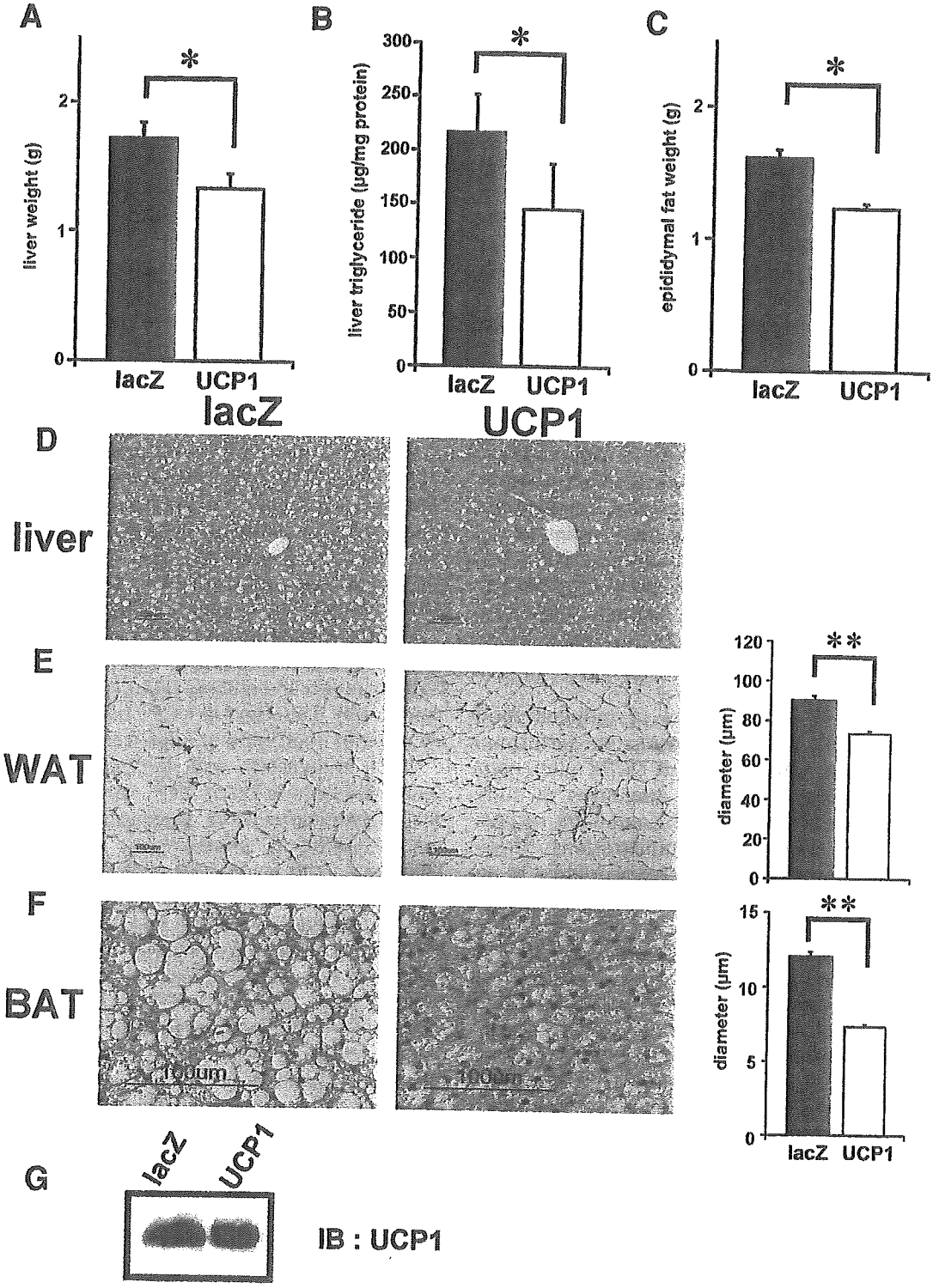

FIG. 2. Hepatic and adipose fat accumulations were decreased in UCP1 mice. Mice were killed after a 10-h fast on day 7 after adenoviral injection, and liver, epididymal fat (WAT), and brown adipose tissues (BAT) were removed. Liver weight (*A*), triglyceride content (*B*), and epididymal fat weight (*C*) were determined (n = 6 per group). *D–F*: Histological findings with hematoxylin and eosin (HE) staining of the liver (*D*), WAT (*E*), and BAT (*F*) in high-fat–fed control (*left*) and UCP1 mice (*middle*). In WAT (*E*) and BAT (*F*) tissues, cell diameters were measured (*right*). *G*: Endogenous UCP1 expression in BAT was compared between control (*left lane*) and UCP1 mice (*right lane*) by immunoblotting (n = 6 per group). Representative histological findings and immunoblots are presented. Data are presented as means ± SE. *P < 0.05, **P < 0.01 assessed by unpaired t test.

cantly decreased in UCP1 mice (Fig. 4*D*). Thus, hepatic UCP1 expression also improved diet-induced dyslipidemia.

Serum insulin levels were markedly decreased, by 57% (Fig. 4*E*), in UCP1 mice, despite lower blood glucose levels (Fig. 1*C*), indicating marked improvement of systemic insulin sensitivity. Serum adiponectin and TNF-α levels were similar in these groups (Fig. 4*F*), suggesting that these adipocytokines are not involved in the improvement of insulin resistance in UCP1 mice. In contrast, serum leptin levels were significantly decreased, by 56%, in

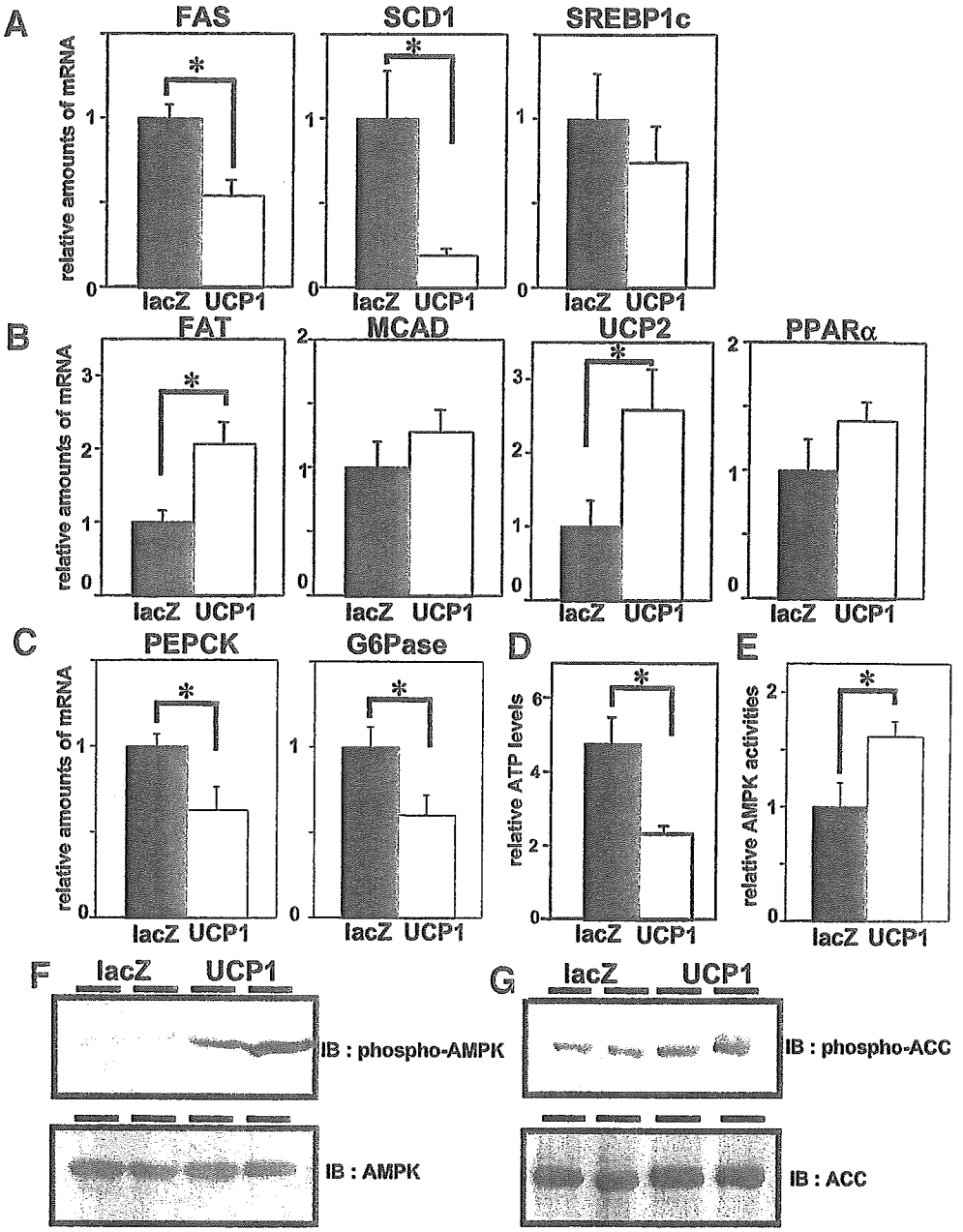

FIG. 3. Hepatic expressions of enzymes involved in lipid metabolism and glucose production and phosphorylations of AMPK and ACC. *A–C*: Relative amounts of mRNA were measured by quantitative RT-PCR and corrected with glyceraldehyde-3-dehydrogenase as the standard. Hepatic total RNA of mice, on day 3 after adenoviral administration in the 10-h–fasted state, was isolated. Expressions of lipogenic enzymes and SREBP1c (*A*), enzymes for fatty acid oxidation and PPAR-α (*B*), and enzymes for hepatic glucose production (*C*) in the liver were assayed (n = 6 per group). *D* and *E*: ATP concentrations (*D*) and AMPK activity (*E*) in the liver were measured. Data are presented as the relative amounts compared with those in standard diet–fed control mice (n = 6 per group). *F* and *G*: Immunoblots using anti–phospho-AMPK (*F*) or anti–phospho-ACC (*G*) antibody (*top*), as well as anti-AMPK (*F*) or anti-ACC1 (*G*) antibody (*bottom*) revealed the phosphorylation state of the AMPK α-subunit in the liver on day 3 after adenoviral injection (n = 2 per group). Data are presented as means ± SE. *P < 0.05 assessed by unpaired t test.

UCP1 mice compared with those in control mice (Fig. 4*F*) concomitantly with decreased food intake (Fig. 1*F*). In control mice that were fed a high-fat diet, marked hyperleptinemia was observed (serum leptin concentrations, standard diet–fed mice versus high-fat diet–fed mice: 0.48 ± 0.08 vs. 32 0.8 ± 4.6 ng/ml) despite increased food intake (compare Fig. 1*F* with Fig. 5*D*), indicating leptin resistance. The present results suggest that hepatic UCP1 expression improves hypothalamic leptin resistance in obese and diabetic mice. To directly test whether leptin sensitivity was improved, we performed leptin tolerance tests (Fig. 4*G*). Leptin was injected intraperitoneally into fasted mice, followed by measurement of 12-h food intakes. The food intake inhibition by leptin administration was far more profound in UCP1 mice than in LacZ mice. Thus, UCP1 mice responded strongly to leptin administration, clearly showing that hepatic UCP1 expression exerts a therapeutic effect on hypothalamic leptin resistance.

Hepatic UCP1 expression exerted minimal effects in standard diet–fed lean mice. Hepatic UCP1 expression reduced body weight and blood glucose and lipid levels in obese and diabetic mice. These are very promising results suggesting that ectopic UCP1 expression may be useful in treating diabetic individuals who are obese. However, if

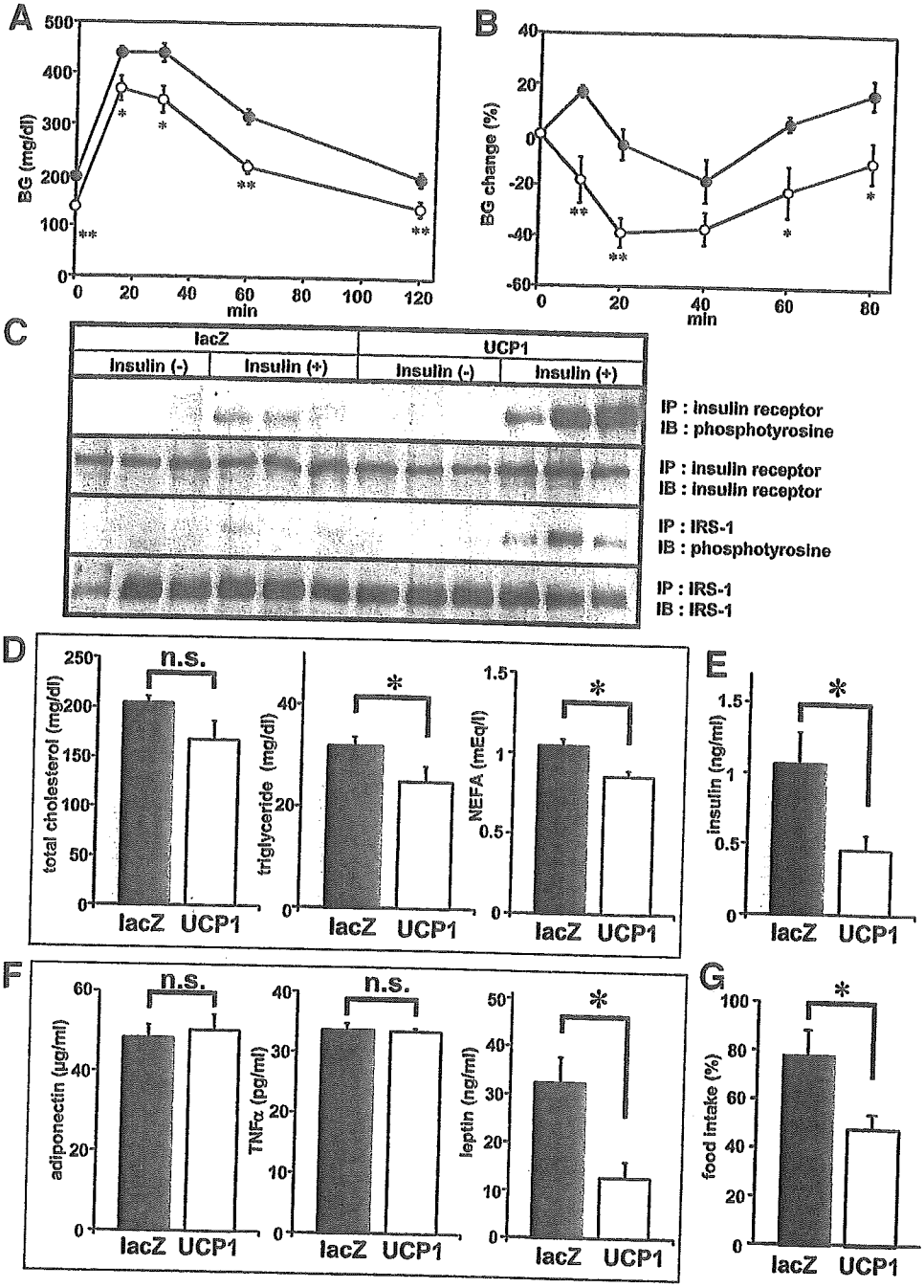

FIG. 4. Hepatic UCP1 expression improved glucose tolerance and insulin sensitivity. *A* and *B*: High-fat–fed mice on day 7 after adenoviral administration were subjected to glucose tolerance (*A*) and insulin tolerance (*B*) tests. Glucose tolerance tests were performed with an oral glucose load (2 g/kg body wt) after a 10-h fast. Insulin tolerance tests were performed in an ad libitum–fed state. Data were expressed as percentages of blood glucose levels immediately before intraperitoneal insulin loading (0.75 units/kg body wt). *C*: Insulin-stimulated tyrosine phosphorylation of insulin receptor and IRS1 proteins in muscle (n = 3 per group). Mice that were fasted for 16 h received an intravenous injection of 100 μl of normal saline with or without insulin (10 units/kg body wt). Hindlimb muscles were removed 300 s later, and lysates were immunoprecipitated with each antibody, as indicated. Immunoprecipitates were subjected to SDS-PAGE and immunoblotted with anti-phosphotyrosine antibody (4G10) or individual antibodies as indicated. *D–F*: Plasma lipid parameters (*D*; *left*, total cholesterol; *middle*, triglyceride; *right*, free fatty acids), serum insulin (*E*), and adipocytokines (*F*; *left*, adiponectin; *middle*, TNF-α; *right*, leptin) of high-fat–fed mice on day 7 after adenoviral administration were measured in the 10-h–fasted state. *G*: Leptin tolerance tests were performed on day 7 after adenoviral administration as described in RESEARCH DESIGN AND METHODS. Data were expressed as ratios to the food intake amounts of vehicle-treated mice (n = 6 per group). Data are presented as means ± SE. *P < 0.05, **P < 0.01 assessed by unpaired t test.

this were also the case in lean individuals, then these individuals would become leaner, possibly even developing malnutrition and hypoglycemia. We therefore performed experiments with a similar design but used 9-week-old standard diet–fed lean mice, i.e., the same age as the high-fat–fed mice.

It is intriguing that although ectopic UCP1 expression levels in the liver were similar under high-fat and standard diet conditions (Fig. 5*A*), the resultant phenotypes were completely different. In standard diet–fed lean mice, hepatic UCP1 expression did not alter body weight (Fig. 5*B*), fasting blood glucose levels (Fig. 5*C*), or food intake

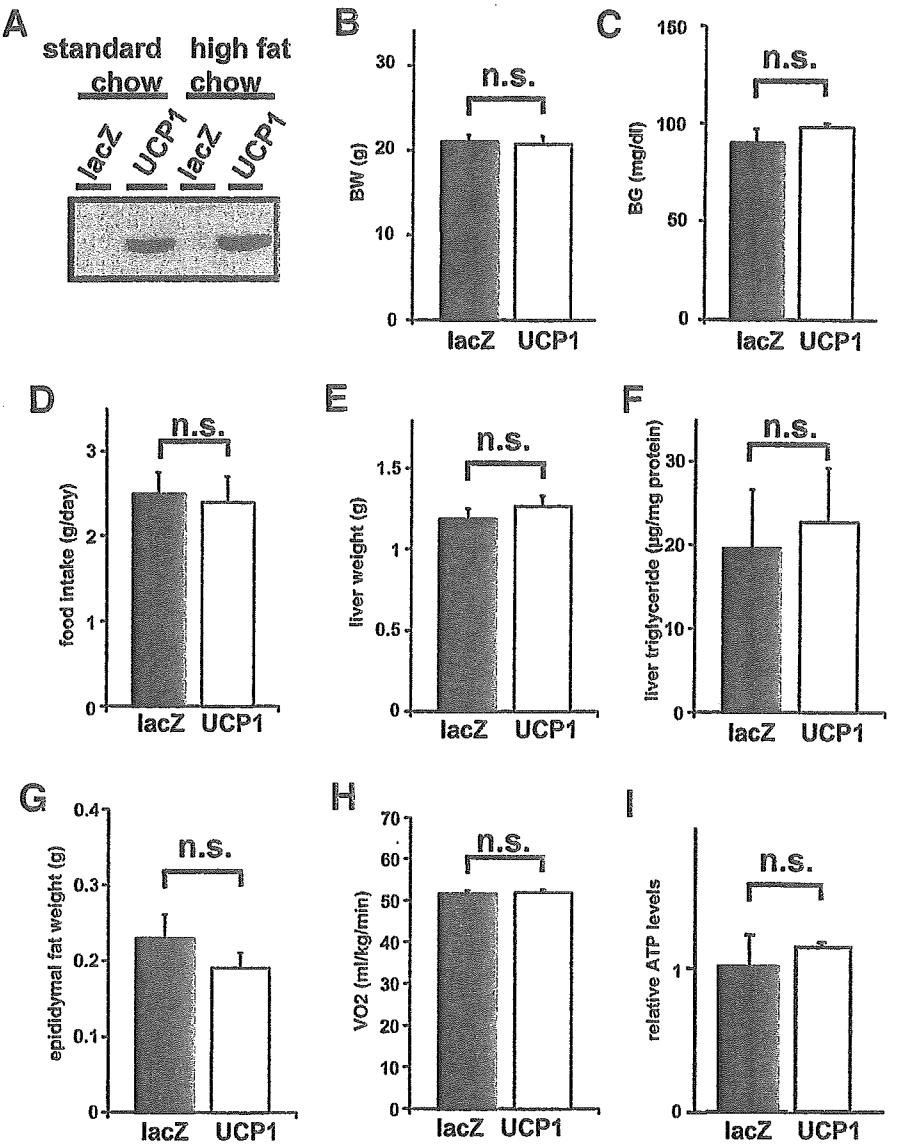

FIG. 5. Minimal effects of hepatic UCP1 expression in standard diet–fed lean mice. *A*: **Hepatic UCP1 expression in standard or high-fat diet–fed mice on day 7 after adenoviral administration at 9 weeks of age. Liver extracts from mice were immunoblotted using anti-UCP1 antibody.** *B* **and** *C*: **Body weights (*B*) and fasting blood glucose levels (*C*) were measured on day 7 after adenoviral injection.** *D*: **Food intake amounts were measured daily, and the average daily food intake for 7 days after adenoviral administration is represented.** *E–G*: **Hepatic weights (*E*), triglyceride contents (*F*), and epididymal fat weights (*G*) were determined ($n = 6$ per group) on day 7 after adenoviral injection.** *H* **and** *I*: **Resting Vo_2 (*H*) and hepatic ATP levels (*I*) were measured in the same way as in previous figures. Hepatic ATP levels are presented as the relative amounts compared with those in standard diet–fed control mice. Data are presented as means ± SE. **$P < 0.01$ assessed by one-factor ANOVA.**

amounts (Fig. 5*D*). In addition, hepatic weight (Fig. 5*E*), triglyceride content (Fig. 5*F*), and epididymal fat weight (Fig. 5*G*) were not changed. Thus, hepatic UCP1 expression did not exert significant effects on glucose metabolism or adiposity in lean mice.

To determine why hepatic UCP1 expression in lean mice did not significantly alter metabolic conditions, we measured basal energy expenditure and hepatic ATP contents. Hepatic UCP1 expression did not significantly change basal energy expenditure (Fig. 5*H*) or hepatic ATP levels (Fig. 5*I*), suggesting that UCP1 ectopically expressed in the liver is minimally involved in mitochondrial uncoupling, when surplus energy is not stored in the liver. Thus, hepatic UCP1 is likely to dissipate excess energy while having no effect on required energy. These characteristics are favorable in terms of therapeutic strategies for the metabolic syndrome.

DISCUSSION

In this study, after mice had developed obesity-associated diabetes, ectopically expressing UCP1 in the liver resulted in marked improvements in both disease conditions. UCP1 expression would be expected to decrease ATP generation in the liver and thus to activate hepatic AMPK. Indeed, ATP contents were decreased, and AMPK and ACC phosphorylations were increased. AMPK reportedly phosphorylates and inactivates ACC, resulting in a decrease in malonyl-CoA generation (21). Because malonyl-CoA is a negative regulator via suppression of CPT1, a rate-limiting enzyme for fatty acid oxidation (22), a decrease in malonyl-CoA generation is likely to enhance fatty acid oxidation to meet respiratory demands. Furthermore, hepatic expressions of lipogenic enzymes were decreased by UCP1 expression in the liver, which may be explained by

AMPK activation and possible SREBP1 reduction in the liver; metformin reportedly activates AMPK and inhibits hepatic SREBP1 expression (23). Taken together, the results suggest that fatty acid synthesis was suppressed with concomitant enhancement of fatty acid oxidation, resulting in the marked decrease in hepatic triglyceride contents.

How might a change in hepatic lipid metabolism affect the energy balance of the entire body? It is noteworthy that the weight and/or cell sizes of epididymal fat and brown adipose tissues were markedly decreased by hepatic UCP1 expression in the present study. Inhibition of fat accumulation in adipose tissues was also observed in UCP1 and in UCP3 transgenic mice under the control of muscle-specific promoters (7,8). Mice lacking ACC2, which is predominantly expressed in the heart and muscle of wild-type mice, also markedly inhibited fat accumulation in their adipose tissues (24). In reports using transgenic models, muscle is a site of increasing energy expenditure, through mitochondrial uncoupling, which prevents obesity. In the present study, hepatic expression of UCP1 reduced fat contents, rather than inhibiting fat accumulation, not only in the liver but also in adipose tissues, indicating promotion of hydrolysis of triglycerides already stored in the adipose tissues. Thus, hepatic uncoupling is likely to convey signals to peripheral adipose tissues. These signals might involve an autonomic nerve network, because the hydrolysis of triglycerides stored in adipose tissues is controlled mainly by the cAMP-mediated pathway, including sympathetic nerve activation (25). Alternatively, a decline in serum fatty acid concentrations, observed in UCP1 mice, or some unknown factors secreted by the liver might trigger lipolysis in adipose tissues. Although more work is required to elucidate the mechanism underlying this remote effect, enhancement of hepatic uncoupling is likely to exert therapeutic, rather than preventive, effects on insulin resistance associated with obesity. Thus, the liver is a potential therapeutic target for diabetes with obesity. Furthermore, unraveling the underlying mechanism may lead to development of antiobesity pharmacological agents that promote lipolysis in adipose tissues.

The present results are also interesting with respect to appetite regulation. Transgenic mice overexpressing UCP3 in skeletal muscle are reportedly hyperphagic (8), whereas UCP1 transgenic mice show no changes in food intake (7). In these transgenic mice, UCPs are continuously overexpressed throughout life, including in the fetal stage. In contrast, the UCP was expressed after development of diabetes with obesity in the present study. In obese subjects, serum leptin levels are reportedly increased with an increment in adipose tissue mass (26,27). Despite increased serum leptin levels, neither appetite nor food intake was suppressed, but instead increased, which is explained by hypothalamic leptin resistance in obese subjects. Herein, control mice on a high-fat diet were hyperphagic compared with those on a standard diet, whereas serum leptin levels were markedly elevated in high-fat diet–fed mice, indicating the development of leptin resistance. It is interesting that hepatic UCP1 expression reversed hyperphagia in high-fat diet–fed mice. Leptin tolerance tests show marked improvement of hypothalamic leptin resistance in UCP1 mice, another remote effect of hepatic UCP1 expression. In addition, increased fatty acid oxidation might be involved in the decreased food intake, because administration of peroxisome proliferator–activated receptor (PPAR)-α agonists reportedly reduces food intake amounts, but not in mice deficient in PPAR-α (28). Furthermore, streptozotocin-induced hyperphagia was reportedly reversed by hepatic expression of protein phosphatase-1 (29), suggesting that altering hepatic metabolism modulates appetite. Vagal pathways from the liver to the brain mediate the fat-induced changes in hypothalamic neuropeptides and feeding behavior in diabetic rats (30). Taken together with these observations, through appetite modulation, the liver also holds promise as a target for treatment of diabetes with obesity.

The most intriguing finding of the present study is that, despite similar UCP1 expression levels in mice on high-fat and standard diets, the resultant phenotypes were completely different. Hepatic UCP1 expression exerted no significant effects on food intake, weight change, or blood glucose levels in standard diet–fed lean mice. No alterations in energy expenditure or hepatic ATP contents were observed with hepatic UCP1 expression, indicating that, in the absence of a significant energy surplus, ectopic UCP1 has minimal effects on mitochondrial uncoupling. We performed similar experiments in a mildly obese and insulin-resistant model, 15% fat-fed mice. In these mice, hepatic UCP1 expression did not change body weight or food intake. Glucose tolerance and insulin sensitivity were significantly improved, but the effects were smaller (data not shown) than those in a more severely obese and insulin-resistant model, 32% fat-fed mice, reported here. Furthermore, under 32% high-fat–fed conditions in the present study, although hepatic UCP1 expression decreased ATP levels in the liver, the reduced ATP concentrations still exceeded those in standard diet–fed mice, suggesting that enhanced expression of UCPs in the liver does not itself produce an energy shortage. Taken together, hepatic UCP1 is likely to sense the metabolic state in the liver and function according to the degree of stored energy in the liver. In the reconstituted system, addition of fatty acids is indispensable for proton transport by UCP1 (31,32). Although the underlying mechanism has been widely debated (33,34), fatty acid cycling seems to be important for proton transport by UCP1 (35,36). Via such a mechanism, ectopic UCP1 activity in the liver may depend on the metabolic state, probably on the amount of stored fat in the liver. Thus, hepatic UCP1 seems to dissipate surplus energy but not to affect required energy. Therefore, the liver, in which intracellularly stored fat changes dramatically according to the energy balance, seems to be a good target tissue for enhanced expression of UCPs. This feature is of particular importance, as applied to therapeutic strategies for type 2 diabetes associated with obesity and insulin resistance.

Recently, it was reported that, using a transgenic technique, skeletal muscle expression of UCP1 in genetically obese mice lowers blood pressure (37), suggesting that uncoupling decreases the risk for atherosclerosis in patients with obesity and type 2 diabetes. In addition, uncoupling reportedly decreases the production of reactive oxygen species (38), although total oxygen consumption

increases. A high mitochondrial electrochemical gradient is associated with the production of reactive oxygen species that may damage tissues, a possible cause of diabetes complications and atherosclerosis (39). Thus, the respiratory uncoupling increment in the liver may protect tissues from oxidative stress. Taken together with the results of the present study, enhancement of UCPs in the liver is a potential therapy for the metabolic syndrome via reductions in adiposity and blood glucose levels as well as possibly reactive oxygen species in obese and diabetic individuals.

ACKNOWLEDGMENTS

This work was supported by a Grant-in-Aid for Scientific Research (B2, 15390282); a Grant-in-Aid for Exploratory Research (15659214); and Tohoku University 21st Century COE Program "Comprehensive Research and Education Center for Planning of Drug Development and Clinical Evaluation" to H.K. and a Grant-in-Aid for Scientific Research (13204062); and Tohoku University 21st Century COE Program "the Center for Innovative Therapeutic Development for Common Diseases" to Y.O. from the Ministry of Education, Science, Sports and Culture of Japan.

We thank Prof. Y. Moriyama (Okayama University) for helpful suggestions for measuring ATP. We also thank I. Sato and K. Kawamura for technical support.

REFERENCES

1. Friedman JM: A war on obesity, not the obese. *Science* 299:856–858, 2003
2. Klingenberg M, Huang SG: Structure and function of the uncoupling protein from brown adipose tissue. *Biochim Biophys Acta* 1415:271–296, 1999
3. Enerback S, Jacobsson A, Simpson EM, Guerra C, Yamashita H, Harper ME, Kozak LP: Mice lacking mitochondrial uncoupling protein are cold-sensitive but not obese. *Nature* 387:90–94, 1997
4. Himms-Hagen J: Brown adipose tissue thermogenesis and obesity. *Prog Lipid Res* 28:67–115, 1989
5. Kopecky J, Clarke G, Enerback S, Spiegelman B, Kozak LP: Expression of the mitochondrial uncoupling protein gene from the aP2 gene promoter prevents genetic obesity. *J Clin Invest* 96:2914–2923, 1995
6. Kopecky J, Hodny Z, Rossmeisl M, Syrovy I, Kozak LP: Reduction of dietary obesity in aP2-Ucp transgenic mice: physiology and adipose tissue distribution. *Am J Physiol* 270:E768–E775, 1996
7. Li B, Nolte LA, Ju JS, Han DH, Coleman T, Holloszy JO, Semenkovich CF: Skeletal muscle respiratory uncoupling prevents diet-induced obesity and insulin resistance in mice. *Nat Med* 6:1115–1120, 2000
8. Clapham JC, Arch JR, Chapman H, Haynes A, Lister C, Moore GB, Piercy V, Carter SA, Lehner I, Smith SA, Beeley LJ, Godden RJ, Herrity N, Skehel M, Changani KK, Hockings PD, Reid DG, Squires SM, Hatcher J, Trail B, Latcham J, Rastan S, Harper AJ, Cadenas S, Buckingham JA, Brand MD, Abuin A: Mice overexpressing human uncoupling protein-3 in skeletal muscle are hyperphagic and lean. *Nature* 406:415–418, 2000
9. Ono H, Shimano H, Katagiri H, Yahagi N, Sakoda H, Onishi Y, Anai M, Ogihara T, Fujishiro M, Viana AY, Fukushima Y, Abe M, Shojima N, Kikuchi M, Yamada N, Oka Y, Asano T: Hepatic Akt activation induces marked hypoglycemia, hepatomegaly, and hypertriglyceridemia with sterol regulatory element binding protein involvement. *Diabetes* 52:2905–2913, 2003
10. Kozak LP, Britton JH, Kozak UC, Wells JM: The mitochondrial uncoupling protein gene: correlation of exon structure to transmembrane domains. *J Biol Chem* 263:12274–12277, 1988
11. Nakazaki M, Kakei M, Ishihara H, Koriyama N, Hashiguchi H, Aso K, Fukudome M, Oka Y, Yada T, Tei C: Association of upregulated activity of K(ATP) channels with impaired insulin secretion in UCP1-expressing insulinoma cells. *J Physiol* 540:781–789, 2002
12. Katagiri H, Asano T, Ishihara H, Inukai K, Shibasaki Y, Kikuchi M, Yazaki Y, Oka Y: Overexpression of catalytic subunit p110α of phosphatidylinositol 3-kinase increases glucose transport activity with translocation of glucose transporters in 3T3-L1 adipocytes. *J Biol Chem* 271:16987–16990, 1996
13. Kanegae Y, Lee G, Sato Y, Tanaka M, Nakai M, Sakaki T, Sugano S, Saito I: Efficient gene activation in mammalian cells by using recombinant adenovirus expressing site-specific Cre recombinase. *Nucleic Acids Res* 23:3816–3821, 1995
14. Ikemoto S, Thompson KS, Takahashi M, Itakura H, Lane MD, Ezaki O: High fat diet-induced hyperglycemia: prevention by low level expression of a glucose transporter (GLUT4) minigene in transgenic mice. *Proc Natl Acad Sci U S A* 92:3096–3099, 1995
15. Ogihara T, Shin BC, Anai M, Katagiri H, Inukai K, Funaki M, Fukushima Y, Ishihara H, Takata K, Kikuchi M, Yazaki Y, Oka Y, Asano T: Insulin receptor substrate (IRS)-2 is dephosphorylated more rapidly than IRS-1 via its association with phosphatidylinositol 3-kinase in skeletal muscle cells. *J Biol Chem* 272:12868–12873, 1997
16. Folch J, Lees M, Sloane Stanley GH: A simple method for the isolation and purification of total lipides from animal tissues. *J Biol Chem* 226:497–509, 1957
17. Manfredi G, Yang L, Gajewski CD, Mattiazzi M: Measurements of ATP in mammalian cells. *Methods* 26:317–326, 2002
18. Sakoda H, Ogihara T, Anai M, Fujishiro M, Ono H, Onishi Y, Katagiri H, Abe M, Fukushima Y, Shojima N, Inukai K, Kikuchi M, Oka Y, Asano T: Activation of AMPK is essential for AICAR-induced glucose uptake by skeletal muscle but not adipocytes. *Am J Physiol Endocrinol Metab* 282:E1239–E1244, 2002
19. Igel M, Becker W, Herberg L, Joost HG: Hyperleptinemia, leptin resistance, and polymorphic leptin receptor in the New Zealand obese mouse. *Endocrinology* 138:4234–4239, 1997
20. Ishigaki Y, Oikawa S, Suzuki T, Usui S, Magoori K, Kim DH, Suzuki H, Sasaki J, Sasano H, Okazaki M, Toyota T, Saito T, Yamamoto TT: Virus-mediated transduction of apolipoprotein E (ApoE)-sendai develops lipoprotein glomerulopathy in ApoE-deficient mice. *J Biol Chem* 275: 31269–31273, 2000
21. Hardie DG: Regulation of fatty acid and cholesterol metabolism by the AMP-activated protein kinase. *Biochim Biophys Acta* 1123:231–238, 1992
22. McGarry JD, Brown NF: The mitochondrial carnitine palmitoyltransferase system: from concept to molecular analysis. *Eur J Biochem* 244:1–14, 1997
23. Zhou G, Myers R, Li Y, Chen Y, Shen X, Fenyk-Melody J, Wu M, Ventre J, Doebber T, Fujii N, Musi N, Hirshman MF, Goodyear LJ, Moller DE: Role of AMP-activated protein kinase in mechanism of metformin action. *J Clin Invest* 108:1167–1174, 2001
24. Abu-Elheiga L, Matzuk MM, Abo-Hashema KA, Wakil SJ: Continuous fatty acid oxidation and reduced fat storage in mice lacking acetyl-CoA carboxylase 2. *Science* 291:2613–2616, 2001
25. Londos C, Brasaemle DL, Schultz CJ, Adler-Wailes DC, Levin DM, Kimmel AR, Rondinone CM: On the control of lipolysis in adipocytes. *Ann N Y Acad Sci* 892:155–168, 1999
26. Maffei M, Halaas J, Ravussin E, Pratley RE, Lee GH, Zhang Y, Fei H, Kim S, Lallone R, Ranganathan S, et al.: Leptin levels in human and rodent: measurement of plasma leptin and ob RNA in obese and weight-reduced subjects. *Nat Med* 1:1155–1161, 1995
27. Considine RV, Sinha MK, Heiman ML, Kriauciunas A, Stephens TW, Nyce MR, Ohannesian JP, Marco CC, McKee LJ, Bauer TL, et al.: Serum immunoreactive-leptin concentrations in normal-weight and obese humans. *N Engl J Med* 334:292–295, 1996
28. Fu J, Gaetani S, Oveisi F, Lo Verme J, Serrano A, Rodriguez De Fonseca F, Rosengarth A, Luecke H, Di Giacomo B, Tarzia G, Piomelli D: Oleylethanolamide regulates feeding and body weight through activation of the nuclear receptor PPAR-alpha. *Nature* 425:90–93, 2003
29. Yang R, Newgard CB: Hepatic expression of a targeting subunit of protein phosphatase-1 in streptozotocin-diabetic rats reverses hyperglycemia and hyperphagia despite depressed glucokinase expression. *J Biol Chem* 278:23418–23425, 2003
30. la Fleur SE, Ji H, Manalo SL, Friedman MI, Dallman MF: The hepatic vagus mediates fat-induced inhibition of diabetic hyperphagia. *Diabetes* 52:2321–2330, 2003
31. Strieleman PJ, Schalinske KL, Shrago E: Fatty acid activation of the reconstituted brown adipose tissue mitochondria uncoupling protein. *J Biol Chem* 260:13402–13405, 1985
32. Winkler E, Klingenberg M: Effect of fatty acids on H+ transport activity of the reconstituted uncoupling protein. *J Biol Chem* 269:2508–2515, 1994
33. Klingenberg M, Echtay KS: Uncoupling proteins: the issues from a biochemist point of view. *Biochim Biophys Acta* 1504:128–143, 2001

34. Jezek P: Possible physiological roles of mitochondrial uncoupling proteins—UCPn. *Int J Biochem Cell Biol* 34:1190–1206, 2002
35. Skulachev VP: Fatty acid circuit as a physiological mechanism of uncoupling of oxidative phosphorylation. *FEBS Lett* 294:158–162, 1991
36. Garlid KD, Orosz DE, Modriansky M, Vassanelli S, Jezek P: On the mechanism of fatty acid-induced proton transport by mitochondrial uncoupling protein. *J Biol Chem* 271:2615–2620, 1996
37. Bernal-Mizrachi C, Weng S, Li B, Nolte LA, Feng C, Coleman T, Holloszy JO, Semenkovich CF: Respiratory uncoupling lowers blood pressure through a leptin-dependent mechanism in genetically obese mice. *Arterioscler Thromb Vasc Biol* 22:961–968, 2002
38. Vidal-Puig AJ, Grujic D, Zhang CY, Hagen T, Boss O, Ido Y, Szczepanik A, Wade J, Mootha V, Cortright R, Muoio DM, Lowell BB: Energy metabolism in uncoupling protein 3 gene knockout mice. *J Biol Chem* 275:16258–16266, 2000
39. Esposito LA, Melov S, Panov A, Cottrell BA, Wallace DC: Mitochondrial disease in mouse results in increased oxidative stress. *Proc Natl Acad Sci U S A* 96:4820–4825, 1999

Available online at www.sciencedirect.com
SCIENCE DIRECT®
Biochemical and Biophysical Research Communications 326 (2005) 402–409
BBRC
www.elsevier.com/locate/ybbrc

Constitutively active PDX1 induced efficient insulin production in adult murine liver

Junta Imai[a,b], Hideki Katagiri[b,*], Tetsuya Yamada[a], Yasushi Ishigaki[a], Takehide Ogihara[b], Kenji Uno[a,b], Yutaka Hasegawa[a,b], Junhong Gao[a,b], Hisamitsu Ishihara[a], Hironobu Sasano[c], Hiroyuki Mizuguchi[d], Tomoichiro Asano[e], Yoshitomo Oka[a]

[a] *Division of Molecular Metabolism and Diabetes, Tohoku University Graduate School of Medicine, Japan*
[b] *Division of Advanced Therapeutics for Metabolic Diseases, Center for Translational and Advanced Animal Research, Tohoku University Graduate School of Medicine, Japan*
[c] *Division of Anatomic Pathology, Tohoku University Graduate School of Medicine, Sendai 980-8575, Japan*
[d] *Division of Cellular and Gene Therapy Products, National Institute of Health Science, Tokyo, Japan*
[e] *Department of Physiological Chemistry and Metabolism, University of Tokyo, Tokyo 113-8655, Japan*

Received 21 October 2004
Available online 19 November 2004

Abstract

To generate insulin-producing cells in the liver, recombinant adenovirus containing a constitutively active mutant of PDX1 (PDX1-VP16), designed to activate target genes without the need for protein partners, was prepared and administered intravenously to streptozotocin (STZ)-treated diabetic mice. The effects were compared with those of administering wild-type PDX1 (wt-PDX1) adenovirus. Administration of these adenoviruses at 2×10^8 pfu induced similar levels of PDX1 protein expression in the liver. While wt-PDX1 expression exerted small effects on blood glucose levels, treatment with PDX1-VP16 adenovirus efficiently induced insulin production in hepatocytes, resulting in reversal of STZ-induced hyperglycemia. The effects were sustained through day 40 when exogenous PDX1-VP16 protein expression was undetectable in the liver. Endogenous PDX1 protein came to be expressed in the liver, which is likely to be the mechanism underlying the sustained effects. On the other hand, albumin and transferrin expressions were observed in insulin-producing cells in the liver, suggesting preservation of hepatocytic functions. Thus, transient expression of an active mutant of PDX1 in the liver induced sustained PDX1 and insulin expressions without loss of hepatocytic function.

Keywords: Insulin; PDX1; Gene therapy; Diabetes; Adenovirus; Transdifferentiation

Type 1 diabetes mellitus is characterized by progressive loss of pancreatic β cells, leading to a lifelong dependency on insulin treatments. Recently, marked advances have been made in transplanting pancreatic islets from human cadavers into type 1 diabetics [1]. However, immune rejection and donor supply are still major challenges in islet cell transplantation. In this context, generation of insulin-producing cells by somatic gene therapy may represent a viable alternative for the treatment for diabetes.

The liver is a possible target organ for generation of insulin-producing cells. Pancreatic and hepatic tissues both express several transcription factors such as HNF1α and C/EBPβ. In addition, these tissues also have similar glucose sensing machinery consisting of the GLUT2 glucose transporter and glucokinase. Furthermore, during embryogenesis, the liver and the ventral pancreas appear to arise from the same cell

* Corresponding author. Fax: +81 22 717 8228.
E-mail address: katagiri-tky@umin.ac.jp (H. Katagiri).

0006-291X/$ - see front matter © 2004 Elsevier Inc. All rights reserved.
doi:10.1016/j.bbrc.2004.11.047

population located within the embryonic endoderm [2]. The gene most likely to be responsible for the difference between the liver and pancreas is pancreatic and duodenal homeobox gene 1 (PDX1), also known as IDX1/IPF1/STF1. PDX1 is expressed in pancreatic buds in the endoderm prior to morphological development of the pancreas [3,4] and has been shown to play a fundamental role in regulating pancreatic development. Gene disruption of PDX1 has been shown to inhibit pancreatic bud maturation and outgrowth, resulting in complete absence of the pancreas [5]. In addition, conditional inactivation of PDX1 in insulin-producing cells results in a progressive loss of β cells, suggesting PDX1 to play an essential role in maintaining β cells [6].

Therefore, to generate insulin-producing cells, several groups have overexpressed PDX1 in various sites [7–11]. Adenovirus-mediated transfer of the PDX1 gene reportedly ameliorates streptozotocin (STZ)-induced hyperglycemia in a short time (within 10 days) [7] as well as for longer periods [12] via production of insulin in the liver. However, helper-dependent adenovirus (HDAD)-mediated PDX1 gene transfer into the liver reportedly results in severe hepatitis and functional failure due to production of pancreatic exocrine enzymes [10]. In addition, transgenic mice overexpressing PDX1 in the liver also develop liver failure [11].

PDX1 has been shown to activate target genes by association with several co-factors such as PBX [13] and the expressions of these protein partners are absent in the liver. To produce a version of PDX1 that would activate target genes without the need for protein partners, the VP16 activation domain from herpes simplex virus was fused to the C-terminus of PDX1 (PDX1-VP16). In PDX1-VP16 transgenic *Xenopus* tadpoles, part or all of the liver is converted to pancreatic tissue, while hepatic differentiation products are lost from the regions converted to pancreas [14].

Therefore, in the present study, we prepared PDX1-VP16 adenovirus and compared the effects of PDX1-VP16 expression with those of wt-PDX1 in the adult murine liver in vivo. These recombinant adenoviruses were administered at a titer of 2×10^8 pfu, which is one to two orders of magnitude lower than those used in previous reports [7,12]. Herein we demonstrate PDX1-VP16 gene transduction to induce hepatocytic production of insulin, but not glucagon or amylase, more efficiently than wt-PDX1, resulting in reversal of STZ-induced hyperglycemia. We found that PDX1-VP16 gene therapy induced endogenous PDX1 expression in the liver, and hence sustained expression of insulin. In contrast to transgenic tadpole experiments, the conversion was partial and liver-specific gene expressions including those of albumin and transferrin were maintained in insulin-producing cells.

Materials and methods

Recombinant adenoviruses. Murine PDX1 cDNA was cloned from a MIN6 cDNA library by PCR. Using PCR, the *ClaI* site was added to murine PDX1 cDNA, which was digested with *ClaI* and subcloned into VP16-N (kind gift from Dr. H. Kanamori) as described [14]. Recombinant adenoviruses containing wt-PDX1 and PDX1-VP16 cDNA were prepared as reported previously [15–17]. LacZ adenovirus was used as a control [18].

Animals. Male C57BL/6N mice were purchased from Clea (Tokyo, Japan), housed in an air-conditioned environment, with a 12-h light-dark cycle, and fed a regular unrestricted diet. Diabetes was induced by intraperitoneal injection of 160–170 mg/kg STZ (Sigma St. Louis, MO) in citrate buffer at 5–6 weeks of age. Blood glucose was determined after a 10 h fast at 6 days after STZ injection; mice with fasting glucose levels of 300–600 mg/dl were used for the experiments. The mice were treated with 2×10^8 plaque-forming units of recombinant adenovirus by systemic injection into the tail vein and killed 40 days after adenovirus injection. Serum insulin concentrations were measured using a rat insulin ELISA Kit Ultra Sensitive (Morinaga, Tokyo, Japan).

Oral glucose tolerance tests. Oral glucose tolerance tests were performed 40 days after adenovirus infusion. Serum glucose levels were determined before, and 15, 30, 60, 90, and 120 min after, administration of oral glucose (1 g/kg body weight).

Immunoblotting. Liver samples were homogenized in buffer (100 mM Tris, pH 8.5, 250 mM NaCl, 1% BP-40, and 1 mM EDTA). Tissue homogenates were centrifuged at 14,000*g* for 10 min at 4 °C. Supernatants including tissue protein extracts (180 μg total protein) were then boiled in Laemmli buffer containing 10 mM dithiothreitol. Aliquots of proteins (15 μg) were subjected to SDS–PAGE. Immunoblot analyses were performed using ECL plus a Western Blotting Detection System Kit (Amersham Buckinghamshire, UK). Antibodies to PDX1 (A-17, Santa Cruz Biotechnology, Santa Cruz, CA) and HSV-1 VP16 (vA-19, Santa Cruz Biotechnology) were commercially obtained.

Immunohistochemistry. Livers of mice were excised 40 days after adenoviral treatment and fixed overnight in 10% paraformaldehyde. Fixed tissues were processed for paraffin embedding and 3 μm sections were prepared. For immunohistochemistry, the streptavidin–biotin (SAB) method was performed using a Histofine SAB-PO kit (Nichirei, Tokyo, Japan) for insulin, glucagon, and amylase, and a MAX-PO kit (Nichirei) for somatostatin, and an EnVision kit/HRP (DAKO, Glostrup, Denmark) for pancreatic polypeptide. Slides were deparaffinized, and then were either autoclaved in citrate buffer for antigen retrieval before being incubated in blocking solution (for amylase, somatostatin, and pancreatic polypeptide detection), or immediately exposed to the blocking solution (for insulin and glucagon detection). For insulin detection, sections were incubated for 18 h at 4 °C with monoclonal antibody against human insulin (Sigma) diluted 1:1000 in PBS. For detection of glucagon, sections were incubated for 18 h at 4 °C with antiserum raised against human glucagon (DAKO) diluted 1:3000 in PBS. For detection of somatostatin, sections were incubated overnight at 4 °C with rat anti-somatostatin monoclonal antibody (Chemicon, Temecula, CA) diluted 1:100 in PBS. For detection of pancreatic polypeptide, sections were incubated overnight at 4 °C with antiserum raised against rat pancreatic polypeptide (LINCO, St. Charles, MO) diluted 1:100 in PBS. For detection of amylase, sections were incubated for 18 h at 4 °C with antiserum raised against the C-terminus of human amylase (Santa Cruz Biotechnology) diluted 1:1000 in PBS. Slides were then incubated with the biotinylated IgG for 1 h and next with peroxidase-conjugated streptavidin for 30 min at room temperature. Finally, immunoreactivity was visualized by incubation with a substrate solution containing 3,3′-diaminobenzidine tetrahydrochloride (DAB).

Fluorescent immunocytochemistry. The 3 μm sections of paraffin-embedded liver were processed as follows. For double staining of

insulin and transferrin or albumin, the sections were incubated overnight with antibodies against insulin and transferrin (goat polyclonal; Santa Cruz Biotechnology) or albumin (rabbit polyclonal; Biogenesis, Kingston, New Hampshire) at 4 °C. Antibodies against insulin, transferrin, and albumin were diluted 1:1000, 1:5000, and 1:5000, respectively, in PBS. For double staining of insulin and transferrin, the sections were then incubated for 1 h at room temperature in a mixture of TRITC-conjugated sheep anti-mouse IgG and FITC-conjugated donkey anti-goat IgG (Jackson Immuno Research, West Grove, PA) diluted 1:1000 in PBS. For double staining of insulin and albumin, the sections were incubated in a mixture of Alexa Fluor 488 goat anti-mose IgG (Molecular Probes, Eugene, OR) and Alexa Fluor 546 goat anti-rabbit IgG diluted 1:1000 in PBS. Sections were observed under a fluorescence microscope (Leica DM RXA, Leica Microsystems, Wetzlar, Germany). The image was analyzed with a Q-fluoro analyzing system (Leica).

Results

To express a PDX1 mutant, in the liver, which is constitutively active without association with protein partners, we prepared a recombinant adenovirus encoding the VP16 activation domain from herpes simplex virus [19,20] fused to the C-terminus of murine PDX1 (PDX1-VP16). For comparison, we also prepared recombinant adenoviruses encoding the wild-type PDX1 (wt-PDX1) and LacZ. These recombinant adenoviruses, at 2×10^8 pfu, were injected intravenously 6 days after STZ administration, when hyperglycemia had already developed; blood glucose levels after a 10 h fast were approximately 400 mg/dl (Fig. 1B). Mice given the LacZ adenovirus were used as controls (LacZ-mice). Systemic infusion of recombinant adenoviruses into mice through the tail vein caused transgene expression primarily in the liver, with no detectable expression in peripheral tissues such as muscle, fat, kidney or brain (data not shown), as reported previously [21].

As shown in Fig. 1A, immunoblotting of hepatic lysates on day 3 after adenoviral administration with anti-PDX1 antibody revealed that ectopic expression of wt-PDX1 or PDX1-VP16 was obtained in the liver. Administration of recombinant adenoviruses at the same titer induced similar levels of PDX1 protein expression.

We next examined the effects of treatment with these adenoviruses on STZ-induced hyperglycemia (Fig. 1B). Administration of wt-PDX1 adenovirus did not significantly decrease fasting blood glucose levels through day 20. Although, interestingly, fasting blood glucose levels were slightly but significantly decreased after day 30 as compared with those in STZ-treated LacZ-mice, administration of wt-PDX1 adenovirus at such a low titer exerted only very small effects in terms of reversal of hyperglycemia.

In contrast, administration of PDX1-VP16 adenovirus more effectively reversed STZ-induced hyperglycemia (Fig. 1B). Hepatic expression of PDX1-VP16 induced significant, profound decreases in fasting blood glucose levels. Although fasting blood glucose levels rose slightly between day 10 and day 15, the therapeutic effects were sustained throughout the experiments. As shown in Table 1, some variation in results was observed. Thirteen percent of PDX1-VP16-mice exhibited almost no decrease in blood glucose levels, although the proportion of these mice was significantly lower than that of wt-PDX1-mice. In contrast, in 27% of PDX1-VP16-mice, fasting blood glucose levels were lower than 200 mg/dl. No such normalization of glucose levels was obtained by wt-PDX1 adenovirus administration (Table 1). Thus, PDX1-VP16 expression in the liver more effectively lowered blood glucose levels and these effects persisted even after adenoviral-mediated gene expression had declined.

To examine the mechanism whereby administration of PDX1-VP16 adenovirus efficiently and persistently lowered blood glucose levels in STZ-treated mice, liver sections from these mice on day 40 after adenoviral administration were immunostained with anti-insulin antibody (Fig. 1C). No insulin staining was detectable in the livers of LacZ-mice. In wt-PDX1-mice, very faint staining with anti-insulin antibody was detected in the liver. In contrast, in PDX1-VP16 mice, strong insulin staining was detected in the cytoplasm of hepatocytes in scattered portions of the liver. The insulin positive cells were seen mostly around vessels. The scant residual insulin-positive cells in the pancreas did not differ significantly among these mice (data not shown). Thus, insulin secretion from hepatocytes is likely to contribute to lowering blood glucose levels in PDX1-VP16-mice.

To confirm that the hepatocytes were secreting insulin, serum levels of immunoreactive insulin in these mice on day 40 after adenoviral administration were measured. In LacZ-mice, STZ treatment induced severe insulinopenia: fasting serum insulin levels were less than 40 pg/ml (Fig. 1D), resulting in severe hyperglycemia. Adenoviral administration of the wt-PDX1 gene slightly increased serum insulin levels. In contrast, PDX1-VP16 adenoviral administration resulted in a substantial increase in serum insulin levels, i.e., more than 6-fold (Fig. 1D). On the other hand, fasting serum insulin levels in the control C57Bl/6N mice of the same age, without STZ treatment, were 340.7 ± 29.9 pg/ml ($n = 6$). Thus, hepatic PDX1-VP16 expression improved fasting serum insulin levels to approximately two-thirds those in normal mice. These data suggest that transient PDX1-VP16 expression in the liver exerted sustained and stronger effects in terms of production and secretion of insulin as compared with wt-PDX1 expression, resulting in the reversal of STZ-induced hyperglycemia.

Oral glucose tolerance tests were performed using LacZ-mice, wt-PDX1-mice, and PDX1-VP16-mice on day 40 (Fig. 2A). STZ-treated LacZ-mice exhibited hyperglycemia: more than 450 mg/dl throughout the

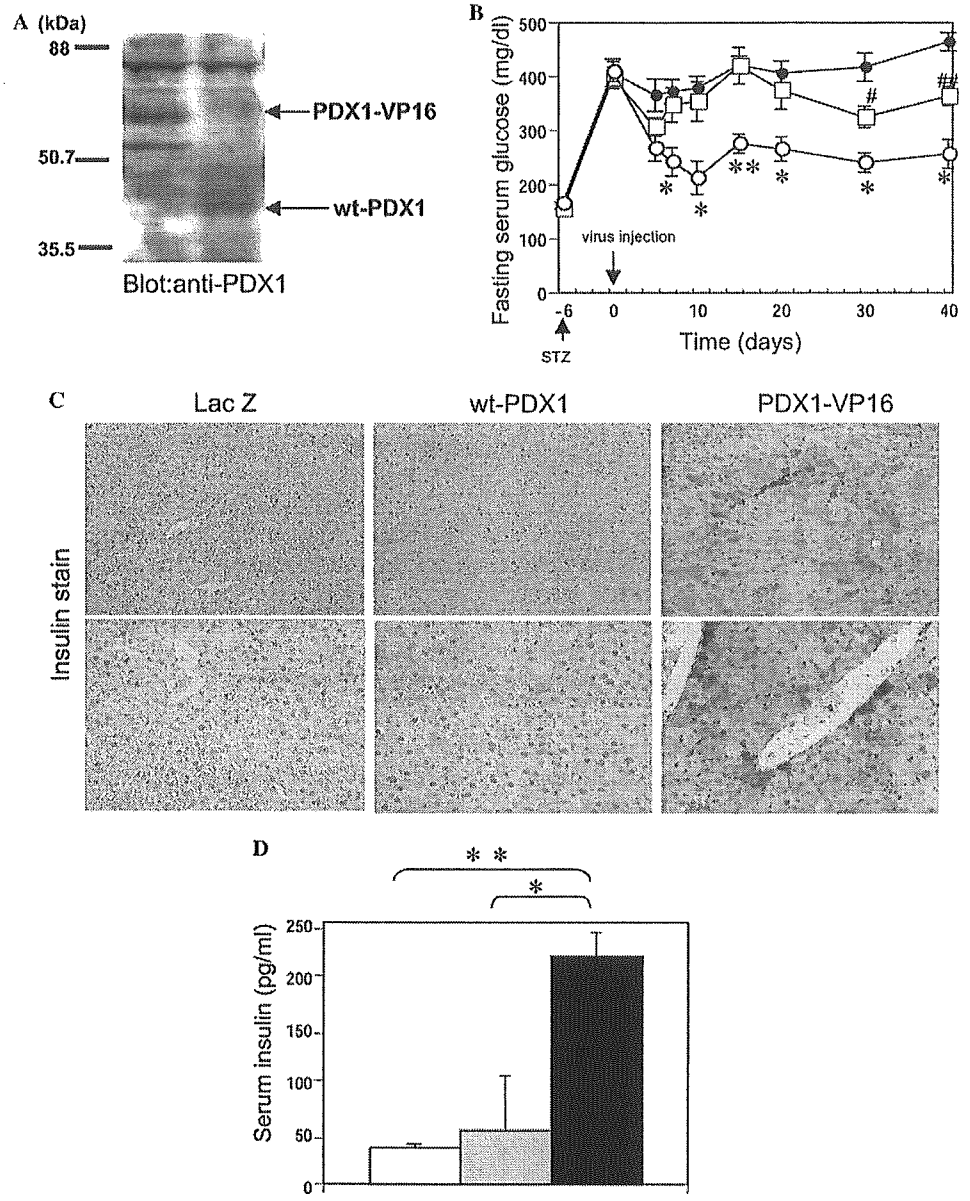

Fig. 1. Effects of wt-PDX1 and PDX1-VP16 adenoviral gene therapy on STZ-induced diabetic mice. (A) Liver lysates from STZ-mice infused with 2×10^8 pfu/body of adenovirus containing wt-PDX1 (left lane) or PDX1-VP16 (right lane) were immunoblotted with anti-PDX1 antibody. (B) Fasting blood glucose levels of STZ-mice treated with LacZ adenovirus (closed circle; $n = 13$), wt-PDX1 adenovirus (open square; $n = 8$) or PDX1-VP16 adenovirus (open circle; $n = 15$). Amount of injected adenoviruses was 2×10^8pfu/body in all experiments. (C) Liver sections from LacZ-mice (left panels), wt-PDX1-mice (middle panels), and PDX1-VP16-mice (right panels) on day 40 after adenoviral treatment were immunostained with anti-insulin antibody. Original magnification 100× (upper panels) and 200× (lower panels). (D) Fasting serum insulin levels 40 days after adenoviral treatment with LacZ (open bar; $n = 7$), wt-PDX1 (gray bar; $n = 8$), or PDX1-VP16 (black bar; $n = 7$) adenovirus. Data are presented as means ± SEM. $^*P < 0.05$, $^{**}P < 0.01$ versus wt-PDX1, $^{\#}p < 0.05$, and $^{\#\#}p < 0.01$ versus LacZ, assessed by unpaired t test.

tests. In PDX1-VP16-mice, glucose levels throughout the tests were significantly lower than those in wt-PDX1-mice. The blood glucose levels peaked at 30 min after glucose load and thereafter tended to fall, although the reversal was incomplete at 120 min. These findings suggest that, in PDX1-VP16-mice, glucose-responsive insulin secretion from the liver is involved in lowering post-prandial blood glucose levels but is not enough to rapidly reverse a rise in blood glucose levels after a glucose load, in contrast to that from the pancreas by β cells.

Using HDAD, PDX1 expression in the liver reportedly induces expression of exocrine enzymes in insulin-producing cells in the liver and causes severe hepatitis. It has also been reported that, in transgenic mice expressing PDX1 ectopically in the liver, not only insulin but

Table 1
Distribution of blood glucose levels in each treatment group

Blood glucose (mg/dl)	100–200	200–300	300–400	400–500	500–600
LacZ (%)	0	0	8	69	23
wt-PDX1 (%)	0	12	50	38	0
PDX1-VP16 (%)	27	47	13	13	0

Blood glucose levels were determined 40 days after each adenoviral treatment. Blood glucose levels of mice before the adenoviral treatment (6 days after STZ injection) were all above 300 mg/dl. (Lac Z; $n = 13$, wt-PDX1; $n = 8$, and PDX1-VP16; $n = 15$.)

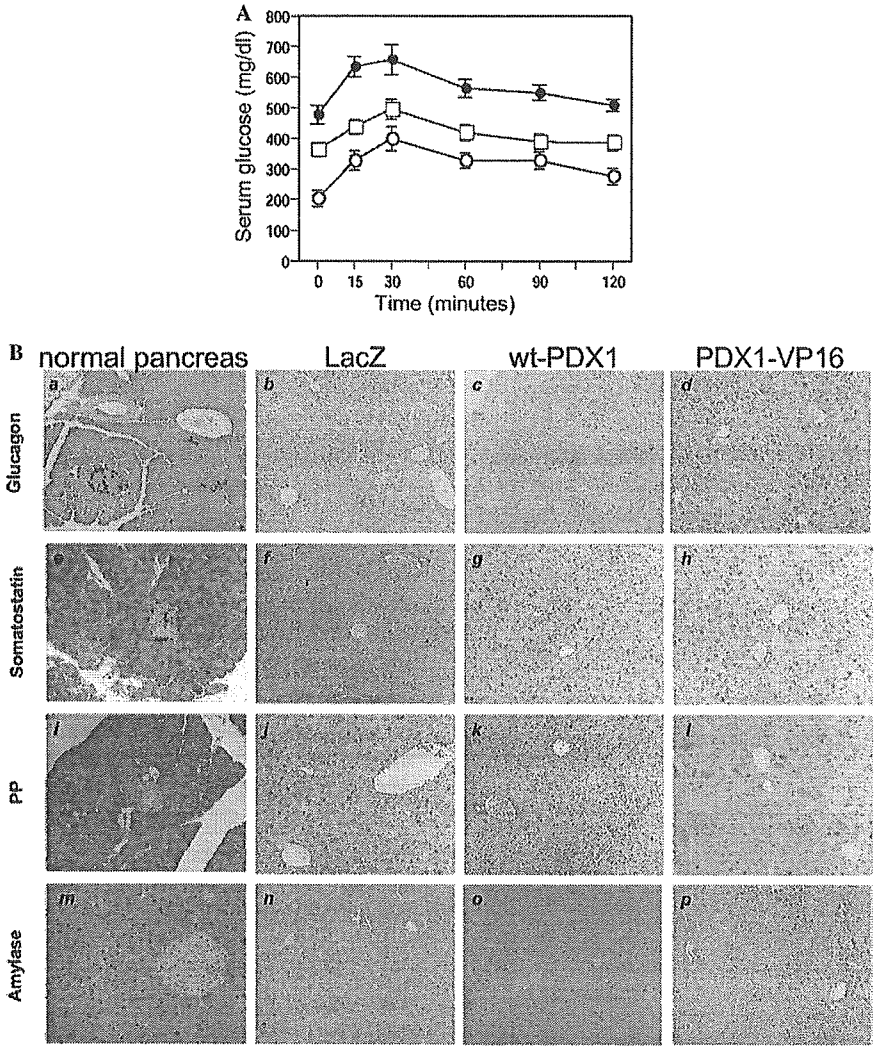

Fig. 2. Effects of wt-PDX1 and PDX1-VP16 adenoviral gene therapy on blood glucose levels after a glucose load, and glucagon, somatostatin, pancreatic polypeptide, and amylase expressions. (A) Blood glucose levels during oral glucose tolerance testing (1 g/kg body weight) in LacZ-mice (closed circle; $n = 7$), wt-PDX1-mice (open square; $n = 8$), and PDX1-VP16-mice (open circle; $n = 7$) on day 40 after adenovirus administration. Data are presented as means ± SEM. (B) immunohistochemical staining of livers from LacZ-mice (b,f,j,n), wt-PDX1-mice (c,g,k,o), and PDX1-VP16-mice (d,h,l,p) with glucagon (b–d), somatostatin (f–h), pancreatic polypeptide (j–l) or amylase (n–p) antibody. Sections of normal pancreas were used as positive controls for each staining procedure (a,e,i,m). Original magnification 100×.

also other endocrine hormones as well as pancreatic exocrine genes are expressed, resulting in dysmorphogenesis and hepatic failure [10]. In contrast, in the present study, adenovirus-mediated transduction of the wt-PDX1 or the PDX1-VP16 gene into the liver did not induce lobe structural abnormalities or substantial infiltration of inflammatory cells (Fig. 2B). Furthermore, using immunohistochemistry, no immunoreactivity against glucagon

or somatostatin was detected in livers from wt-PDX1-mice and PDX1-VP16-mice. In addition, in these livers there was no detectable production of amylase, a pancreatic exocrine enzyme (Fig. 2B), which may explain the normal morphogenesis in our experimental animals. On the other hand, pancreatic polypeptide was expressed in livers from PDX1-VP16-mice, and in those from wt-PDX1-mice though to a lesser extent. These results demonstrate that transient expression of PDX1-VP16 alters the character of hepatocytes to preferentially produce insulin and pancreatic polypeptide, but not other endocrine hormones or exocrine enzymes.

Adenoviral gene transfer induced gene expression for 1 week but, after 2 weeks, this expression reportedly disappeared [22]. However, in the present study, the blood glucose lowering effects and hepatic insulin expression persisted for at least 40 days. Therefore, the time course of PDX1 protein expression levels was examined. As shown in Fig. 3A, immunoblotting using anti-VP16 activation domain antibody revealed PDX1-VP16 protein to be expressed on day 3 but expression was markedly decreased on day 7, and undetectable on day 21. Thus, even after disappearance of VP16-PDX1 expression, hepatocytes expressed insulin, resulting in lowering of blood glucose levels. Interestingly, immunoblotting using anti-PDX1 antibody showed that endogenous PDX1 protein, which had the same molecular weight as wt-PDX1, came to be expressed on day 21. Thus, transient expression of PDX1-VP16 endowed hepatocytes with certain pancreatic β cell features and endogenous PDX1 expression is likely to maintain the insulin-producing function of these cells.

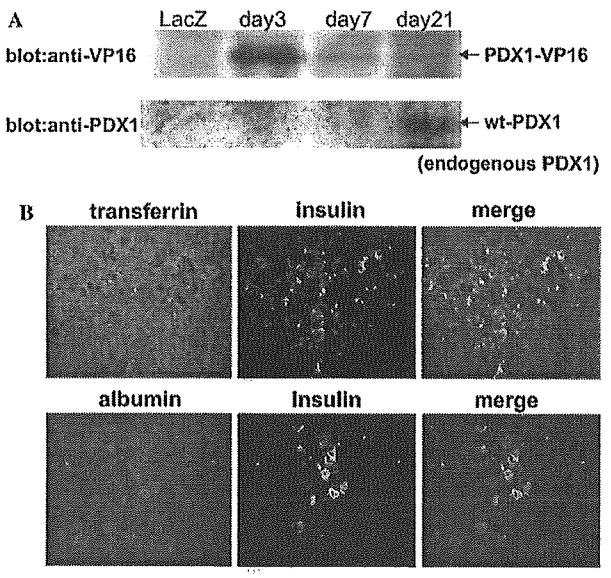

Fig. 3. Treatment with PDX1-VP16 adenovirus induced persistent expression of endogenous PDX1 but albumin and transferrin were co-expressed in insulin-expressing cells. (A) Liver lysates from PDX1-VP16 mice at different time points after adenoviral treatment were immunoblotted with anti-VP16 (upper panel) or anti-PDX1 (lower panel) antibody. (B) Liver sections from PDX1-VP16 mice on day 40 were double-immunostained with insulin (middle panels) and transferrin (upper-left panels) or albumin (lower-left panels) antibodies. Right panels represent the merged images.

To determine whether the insulin-producing cells in the liver had completely transdifferentiated and lost their hepatocytic character, liver sections from PDX1-VP16 mice on day 40 were immunostained with insulin and transferrin (upper panels in Fig. 3B) or albumin (lower panels in Fig. 3B). Fluorescence immunohistochemistry revealed that insulin-producing cells in the liver also expressed transferrin and albumin. Expression levels of these liver-specific proteins were not substantially decreased as compared with non-insulin-producing cells around the insulin-producing cells. These findings suggest functional hepatocyte-specific characteristics are maintained in insulin-producing cells in the liver. Thus, these hepatocytes were not completely converted to pancreatic cells.

Discussion

In the present study, administration of recombinant adenovirus containing an activated form of PDX1 efficiently induced insulin production in hepatocytes, resulting in reversal of STZ-induced hyperglycemia. The effects were sustained even when exogenous protein expression was no longer detectable. In turn, endogenous PDX1 protein came to be expressed in hepatocytes, which is likely to be the mechanism underlying the sustained effects. On the other hand, albumin and transferrin expressions were observed in insulin-producing cells, suggesting the maintenance of hepatocyte-specific characteristics.

Ferber et al. [7] reported that administration of wt-PDX1 adenovirus at 2×10^9 pfu/mouse ameliorates STZ-induced hyperglycemia but the observed period was very short (no more than 10 days). The same research group also reported the long-term effects of PDX1 gene transfer but the titer of recombinant adenovirus used was relatively high ($1–5 \times 10^{10}$ pfu/mouse) [12]. Such high titers may result in liver damage due to adenoviral toxicity. In the present study, to avoid adenoviral toxicity, recombinant adenoviruses were injected at a titer as low as 2×10^8 pfu. With such a small adenoviral delivery, the wt-PDX1 adenovirus exerted very small effects on insulin and glucose levels, whereas PDX1-VP16 adenovirus substantially increased insulin levels and reversed STZ-induced hyperglycemia. These findings suggest that constitutive activation of PDX1 overcomes the inefficiency associated with low expression levels of PDX1 proteins. Thus, adenoviral transfer of the PDX1-VP16 gene into the liver would presumably be safer than wt-PDX1 gene therapy.

HDAD-mediated PDX1 expression in the liver reportedly causes severe hepatitis including marked inflammatory cell infiltration with focal necrosis associated with expression of pancreatic exocrine genes [10]. In addition, conditional transgenic mice generated by crossing CAG-CAT-PDX1 mice with alb-Cre recombinase-mice also displayed functional liver failure with hepatic expression of exocrine enzymes [11]. In these two models, exogenous PDX1 expression is persistent. Transgenes delivered by HDADs are expressed for long periods exceeding several months. In conditional transgenic mice [11], cells, in which the albumin promoter had once been activated, permanently expressed PDX1 driven by the CAG promoter. These findings suggest that high and persistent expression of PDX1 induces exocrine enzyme expression and thereby liver failure. In the present study, exogenous gene expressions of wt-PDX1 and PDX1-VP16 were transient and expression levels were relatively low on day 7 (Fig. 3A). Thus, transient expression appears to be important for endowing hepatocytes with certain features of pancreatic β cells, but not of exocrine cells.

It is noteworthy that exogenous, transient expression of PDX1-VP16 induced prolonged expression of endogenous PDX1 which apparently contributed to persistent insulin production with hepatocytic features. Ber et al. also reported that rat PDX1 gene transduction using first-generation adenovirus induced persistent endogenous (murine) PDX1 expression. Thus, transient expression of wt-PDX1, and more efficiently PDX1-VP16, may induce persistent and low-level expression of endogenous PDX1. In the adult pancreas, persistent but low-level expression of PDX1 is detected only in β cells [3] and PDX1 expression is required for maintaining normal pancreatic β cell function [6]. These observations suggest that persistent, low-level expression of PDX1 is involved in preferential production of insulin and pancreatic popypeptide in hepatocytes.

In transgenic *Xenopus* tadpoles expressing Xlhbox8 (*Xenopus* homolog of PDX1) carrying the VP16 activation domain under a transthyretin promoter, part or all of the liver is reportedly converted to pancreatic tissue without expression of liver-specific gene products, suggesting complete conversion of hepatocytes to pancreatic cells [14]. In contrast, in the present study, insulin-producing cells in the liver in PDX1-VP16 mice also expressed albumin and transferrin, which suggests preservation of hepatocytic functions. This discrepancy may be explained by the differences between amphibian and mammalian cells. Alternatively, the conversion may occur during embryonic differentiation, while, in adult and differentiated hepatocytes, complete transdifferentiation into pancreatic endocrine or exocrine cells would be difficult to achieve even with PDX1-VP16 expression. Although intensive research is necessary to unravel the precise mechanisms underlying transdifferentiation, the partial conversion induced by PDX1-VP16 expression in adult hepatocytes has practical applications, since loss of hepatocytic functions may result in liver failure. Furthermore, incomplete transdifferentiation could prevent the generated insulin-producing cells from being attacked by a destructive autoimmune response in type 1 diabetics.

Acknowledgments

We thank Dr. H. Kanamori (University of Tokyo) for the generous gift of the VP16 gene. We also thank Ms. I. Sato, K. Kawamura, and M. Hoshi for technical support. This work was supported by a Grant-in-Aid for Scientific Research (B2, 15390282), a Grant-in-Aid for Exploratory Research (15659214) to H. Katagiri, and a Grant-in-Aid for Scientific Research (13204062) to Y. Oka from the Ministry of Education, Science, Sports and Culture of Japan. This work was also supported by Tohoku University 21st Century COE Program "CRESCENDO" to J. Imai, J. Gao, and H. Katagiri.

References

[1] A.M. Shapiro, J.R. Lakey, E.A. Ryan, G.S. Korbutt, E. Toth, G.L. Warnock, N.M. Kneteman, R.V. Rajotte, Islet transplantation in seven patients with type 1 diabetes mellitus using a glucocorticoid-free immunosuppressive regimen, N. Engl. J. Med. 343 (2000) 230–238.

[2] G. Deutsch, J. Jung, M. Zheng, J. Lora, K.S. Zaret, A bipotential precursor population for pancreas and liver within the embryonic endoderm, Development 128 (2001) 871–881.

[3] H. Ohlsson, K. Karlsson, T. Edlund, Ipf1, a homeodomain-containing transactivator of the insulin gene, EMBO J. 12 (1993) 4251–4259.

[4] M.F. Offield, T.L. Jetton, P.A. Labosky, M. Ray, R.W. Stein, M.A. Magnuson, B.L. Hogan, C.V. Wright, Pdx-1 is required for pancreatic outgrowth and differentiation of the rostral duodenum, Development 122 (1996) 983–995.

[5] J. Jonsson, L. Carlsson, T. Edlund, H. Edlund, Insulin-promoter-factor 1 is required for pancreas development in mice, Nature 371 (1994) 606–609.

[6] U. Ahlgren, J. Jonsson, L. Jonsson, K. Simu, H. Edlund, Beta-cell-specific inactivation of the mouse ipf1/pdx1 gene results in loss of the beta-cell phenotype and maturity onset diabetes, Genes Dev. 12 (1998) 1763–1768.

[7] S. Ferber, A. Halkin, H. Cohen, I. Ber, Y. Einav, I. Goldberg, I. Barshack, R. Seijffers, J. Kopolovic, N. Kaiser, A. Karasik, Pancreatic and duodenal homeobox gene 1 induces expression of insulin genes in liver and ameliorates streptozotocin-induced hyperglycemia, Nat. Med. 6 (2000) 568–572.

[8] A. Grapin-Botton, A.R. Majithia, D.A. Melton, Key events of pancreas formation are triggered in gut endoderm by ectopic expression of pancreatic regulatory genes, Genes Dev. 15 (2001) 444–454.

[9] R.S. Heller, D.A. Stoffers, M.A. Hussain, C.P. Miller, J.F. Habener, Misexpression of the pancreatic homeodomain protein idx-1 by the hoxa-4 promoter associated with agenesis of the cecum, Gastroenterology 115 (1998) 381–387.

[10] H. Kojima, M. Fujimiya, K. Matsumura, P. Younan, H. Imaeda, M. Maeda, L. Chan, Neurod-betacellulin gene therapy induces islet neogenesis in the liver and reverses diabetes in mice, Nat. Med. 9 (2003) 596–603.
[11] T. Miyatsuka, H. Kaneto, Y. Kajimoto, S. Hirota, Y. Arakawa, Y. Fujitani, Y. Umayahara, H. Watada, Y. Yamasaki, M.A. Magnuson, J. Miyazaki, M. Hori, Ectopically expressed pdx-1 in liver initiates endocrine and exocrine pancreas differentiation but causes dysmorphogenesis, Biochem. Biophys. Res. Commun. 310 (2003) 1017–1025.
[12] I. Ber, K. Shternhall, S. Perl, Z. Ohanuna, I. Goldberg, I. Barshack, L. Benvenisti-Zarum, I. Meivar-Levy, S. Ferber, Functional, persistent, and extended liver to pancreas transdifferentiation, J. Biol. Chem. 278 (2003) 31950–31957.
[13] S. Dutta, M. Gannon, B. Peers, C. Wright, S. Bonner-Weir, M. Montminy, Pdx:Pbx complexes are required for normal proliferation of pancreatic cells during development, Proc. Natl. Acad. Sci. USA 98 (2001) 1065–1070.
[14] M.E. Horb, C.N. Shen, D. Tosh, J.M. Slack, Experimental conversion of liver to pancreas, Curr. Biol. 13 (2003) 105–115.
[15] H. Mizuguchi, M.A. Kay, Efficient construction of a recombinant adenovirus vector by an improved in vitro ligation method, Hum. Gene Ther. 9 (1998) 2577–2583.
[16] H. Mizuguchi, M.A. Kay, A simple method for constructing e1- and e1/e4-deleted recombinant adenoviral vectors, Hum. Gene Ther. 10 (1999) 2013–2017.
[17] T. Anno, S. Uehara, H. Katagiri, Y. Ohta, K. Ueda, H. Mizuguchi, Y. Moriyama, Y. Oka, Y. Tanizawa, Overexpression of constitutively activated glutamate dehydrogenase induces insulin secretion through enhanced glutamate oxidation, Am. J. Physiol. Endocrinol. Metab. 286 (2004) E280–E285.
[18] H. Katagiri, T. Asano, H. Ishihara, K. Inukai, Y. Shibasaki, M. Kikuchi, Y. Yazaki, Y. Oka, Overexpression of catalytic subunit p110alpha of phosphatidylinositol 3-kinase increases glucose transport activity with translocation of glucose transporters in 3t3-l1 adipocytes, J. Biol. Chem. 271 (1996) 16987–16990.
[19] I. Sadowski, J. Ma, S. Triezenberg, M. Ptashne, Gal4-vp16 is an unusually potent transcriptional activator, Nature 335 (1988) 563–564.
[20] S.J. Triezenberg, R.C. Kingsbury, S.L. McKnight, Functional dissection of vp16, the trans-activator of herpes simplex virus immediate early gene expression, Genes Dev. 2 (1988) 718–729.
[21] Y. Ishigaki, S. Oikawa, T. Suzuki, S. Usui, K. Magoori, D.H. Kim, H. Suzuki, J. Sasaki, H. Sasano, M. Okazaki, T. Toyota, T. Saito, T.T. Yamamoto, Virus-mediated transduction of apolipoprotein e (apoe)-sendai develops lipoprotein glomerulopathy in apoe-deficient mice, J. Biol. Chem. 275 (2000) 31269–31273.
[22] M.J. Peeters, G.A. Patijn, A. Lieber, L. Meuse, M.A. Kay, Adenovirus-mediated hepatic gene transfer in mice: comparison of intravascular and biliary administration, Hum. Gene Ther. 7 (1996) 1693–1699.

JOURNAL OF CELLULAR PHYSIOLOGY 202:536–553 (2005)

PKC Mediates Cyclic Stretch-Induced Cardiac Hypertrophy Through Rho Family GTPases and Mitogen-Activated Protein Kinases in Cardiomyocytes

JING PAN,[1]* UGRA S. SINGH,[1] TOSHIYUKI TAKAHASHI,[1] YOSHITOMO OKA,[2] ANTS PALM-LEIS,[1] BRADLEY S. HERBELIN,[1] AND KENNETH M. BAKER[1]

[1]*Division of Molecular Cardiology, Cardiovascular Research Institute, The Texas A&M University System Health Science Center, College of Medicine, Temple, Texas*

[2]*Division of Molecular Metabolism and Diabetes, Department of Internal Medicine, Tohoku University Graduate School of Medicine, Sendai, Japan*

Signaling events, including Rho GTPases and protein kinase C (PKC), are involved in cardiac hypertrophy. However, the mechanisms by which these pathways cooperate during the hypertrophic process remain unclear. Using an in vitro cyclic stretch model with neonatal rat cardiomyocytes, we demonstrated that stretch-induced activation of RhoA, Rac1/Cdc42, and phosphorylation of Rho-guanine nucleotide dissociation inhibitor (GDI) were prevented by inhibition or depletion of PKC, using chelerythrine and phorbol 12-myristate 13-acetate, indicating that phorbol ester-sensitive PKC isozymes may be upstream regulators of Rho GTPases. Using adenoviral-mediated gene transfer of wild-type (WT) and dominant-negative (DN) mutants of PKCα and δ, we found that stretch-induced activation of Rho GTPases and phosphorylation of Rho-GDI were mainly regulated by PKCα. PKCδ was involved in regulation of the activation of Rac1. Stretch-induced increases in [^{3}H]-leucine incorporation, myofibrillar reorganization and cell size, were blocked by inhibition of Rho GTPases, or overexpression of DN PKCα and δ, suggesting that PKCα and δ are both required in stretch-induced hypertrophy, through Rho GTPases-mediated signaling pathways. The mechanism, whereby PKC and Rho GTPases regulate hypertrophy, was associated with mitogen-activated protein (MAP) kinases. Stretch-stimulated phosphorylation of MEK1/ERK1/2 and MKK4/JNK was inhibited by overexpression of DN PKCα and δ, and that of MKK3/p38 inhibited by DN PKCδ. The phosphorylation of ERK and JNK induced by overexpression of WT PKCα, and the phosphorylation of p38 induced by WT PKCδ, were regulated by Rho GTPases. This study represents the first evidence that PKCα and δ are important regulators in mediating activation of Rho GTPases and MAP kinases, in the cyclic stretch-induced hypertrophic process. J. Cell. Physiol. 202: 536–553, 2005. © 2004 Wiley-Liss, Inc.

Mechanical stretch is a major initiating factor for cardiac hypertrophy (Cooper et al., 1985; Komuro et al., 1990; Sadoshima et al., 1992), which evokes various intracellular signaling pathways, such as Rho family GTPases, protein kinase C (PKC), tyrosine kinases, and mitogen-activated protein (MAP) kinase cascades (Sadoshima and Izumo, 1993; Yamazaki et al., 1993; Pan et al., 1999). Although various intracellular signals have been identified, little is known about the potential interplay between these signaling pathways.

The Rho family GTPases, which include RhoA, Rac1, and Cdc42, have been implicated in the regulation of a number of biological processes including cell morphology, motility, adhesion, and growth (Cox et al., 1997; Hall, 1998; Nobes and Hall, 1999). The major function of Rho GTPases is to regulate the assembly and the organization of the actin cytoskeleton (Ridley and Hall, 1992). Cardiac hypertrophy is associated with cell growth and changes in the cytoskeleton and myofibrillar apparatus. Reports indicate that RhoA, Rac1, and Cdc42 are involved in modulating cardiac hypertrophy (Aoki et al., 1998; Pracyk et al., 1998; Aikawa et al., 1999; Nagai et al., 2003). However, the mechanism of

Contract grant sponsor: National Institutes of Health; Contract grant numbers: HL-44883, HL-58439.

*Correspondence to: Jing Pan, Assistant Professor, Cardiovascular Research Institute, The Texas A&M University System Health Science Center, 1901 South 1st Street, Building 205, Temple, TX 76504. E-mail: jpan@medicine.tamu.edu

Received 7 January 2004; Accepted 14 May 2004

DOI: 10.1002/jcp.20151

activation of Rho GTPases has not been well characterized. RhoA activates several protein kinases, including protein kinase N (PKN) and Rho kinases (ROCK2 and ROCK1) (Ishizaki et al., 1996; Watanabe et al., 1996). It has been demonstrated that both PKN and Rho kinase are involved in the Rho-induced hypertrophic response (Morissette et al., 2000; Yanazume et al., 2002). Rac1 promotes activation of ERK, JNK, and p38-MAPK via PAK1 (Zhang et al., 1995; Nosaka et al., 2001; Schmitz et al., 2001). In cardiac myocytes, Rac1 cooperates with c-Raf to promote ERK activation and ANF expression (Clerk et al., 2001).

Rho GTPases cycle between a GDP-bound inactive form and a GTP-bound active form, a process regulated by guanine nucleotide exchange factors (GEFs), which catalyze the exchange of GDP for GTP (Cerione and Zheng, 1996); GTPase activating proteins, which stimulate hydrolysis of GTP to GDP (Lamarche and Hall, 1994); and guanine nucleotide dissociation inhibitors (GDIs), which inhibit the dissociation of GDP from Rho GTPases (Fukumoto et al., 1990). The dissociation of GDI is a prerequisite for membrane association and activation of Rho GTPases by GEFs (Bokoch et al., 1994). The mechanism of the release of Rho-GDI from Rho GTPases remains unclear; but likely involves phosphatidylinositols and the ERM family of proteins (ezrin, radixin, and moesin) (Faure et al., 1999; Mammoto et al., 2000). The structure of Rho-GDI contains sequences for phosphorylation by serine/threonine kinases, which raises the possibility that phosphorylation of GDI promotes release of GDI from Rho GTPases (Olofsson, 1999). It has been reported that PKC regulates thrombin-induced activation of RhoA, through phosphorylation of Rho-GDI, suggesting that GDI phosphorylation may be required for activation of Rho GTPases (Mehta et al., 2001).

PKC consists of a family of serine/threonine kinases, which regulate intracellular signaling and mediate cell proliferation, differentiation, and rearrangement of the cytoskeleton (Nishizuka, 1992; Keenan and Kelleher, 1998). PKC isoforms are divided into three subgroups as follows: the "conventional" (cPKC) α, βI, βII, and γ; the "novel"(nPKC) δ, ε, η, and θ; and the "atypical"(aPKC) ζ, λ, and ι isozymes. Using transgenic mice and adenoviral-mediated overexpression, studies have demonstrated that PKCα and ε are involved in agonist-induced hypertrophic gene expression and growth (Mende et al., 1999; Takeishi et al., 2000; Strait et al., 2001; Braz et al., 2002; Kerkela et al., 2002). The role of PKCδ in cardiac hypertrophy has not been well characterized. Reports have shown that PKCδ expression/activation is increased in cardiac hypertrophy in vivo (Strait and Samarel, 2000; Chen et al., 2001; Braun et al., 2002, 2003), and may also be involved in apoptosis (Chen et al., 2001; Simonis et al., 2002). Mechanical stretch-induced cardiac hypertrophy is also regulated by PKC (Kashiwagi et al., 1998; Seko et al., 1999). However, direct evidence implicating a specific PKC isozyme, as a dominant regulator of stretch-induced hypertrophy, is lacking. PKC and Rho GTPases both have effects on the actin cytoskeleton and activation of MAPK pathways (Ridley and Hall, 1992; Hall, 1998; Keenan and Kelleher, 1998; Toker, 1998). Studies that have directly linked PKC and Rho GTPases signaling suggest significant crosstalk between these two pathways (Nozu et al., 1999; Coghlan et al., 2000; Slater et al., 2001). The targets and signaling pathways shared by Rho GTPases and PKC directed our focus in determining whether these two pathways cooperate in mediating the hypertrophic process.

In the present study, we demonstrated that cyclic stretch-induced activation of Rho GTPases is mediated by PKC (especially PKCα and δ), which by phosphorylating Rho-GDI, regulates the activation of Rho GTPases, and MAP kinase pathways. Our data suggest that the interconnectivity of PKC, Rho GTPases, and MAP kinases has an important role in cyclic stretch-induced cardiac hypertrophy.

MATERIALS AND METHODS

Materials

Monoclonal antibodies against RhoA, Cdc42, polyclonal antibodies against PKCα, ε, δ, ζ, Rho-GDI, ERK1/2, JNK1, p38MAPK, MBP, c-jun, ATF-2, actin and GST-ATF2, c-jun were from Santa Cruz Biotechnology (San Diego, CA). A monoclonal antibody against Rac1 was from Transduction Laboratories (San Jose, CA). Specific phospho-MEK1, MEK3, MEK4, ERK1/2, JNK, and p38 antibodies were from Cell Signaling Technology (Beverly, MA). C3 exoenzyme, Toxin B, and chelerythrine chloride were from Calbiochem (San Diego, CA). [γ-^{32}P]ATP, [α-^{32}P]dCTP, ^{32}P, and [^{3}H]-Leucine were from Perkin Elmer Life Sciences (Boston, MA). Rat ANP and c-fos plasmid was kindly provided by Dr. Fukuda (Keio University, Tokyo, Japan). Other reagents were purchased from Sigma Chemical Co (St. Louis, MO).

Cell culture of cardiomyocytes

Neonatal cardiomyocytes were prepared from the ventricles of 1-day-old Sprague–Dawley rats, as previously described (Kodama et al., 1997) and were cultured in 10% horse serum and 5% fetal bovine serum for 24 h at a density of 1.5×10^5 cells/cm^2 in laminin-coated six-well BioFlex culture plates (Flex cell International Corporation, PA). After 48 h, serum-starved cells were subjected to cyclic stretch using the Flexcell 3000 Strain Unit. The vacuum produced a 15% elongation on the flexible bottom membranes at a frequency of 60 cycles/min. Culture plates not subjected to cyclic stretch were used as controls.

Adenovirus generation

The replication-defective adenovirus-encoding wild-type (WT) or dominant negative mutants of PKCα and δ were gifts from Dr. Yoshitomo Oka (Sendai, Japan). The dominant negative PKCα (AdPKCαdn) and PKCδ (AdPKCδdn) cDNAs consisted of a lysine to arginine mutation in the ATP binding domain at amino acid position 368 and 376, respectively. Each recombinant adenovirus was plaque purified, and amplified using HEK293 cells. The multiplicity of viral infection (moi) for each virus was determined by dilution assay in HEK293 cells. Cardiomyocytes were infected with each adenovirus at a moi of 50 pfu for 6 h at 37°C. Subsequently, the cells were cultured in serum-free DMEM/F12 media for an additional 24 h before treatments or analysis.